

ELECTRONIC SUPPLEMENTARY INFORMATION

for

A New Supramolecular Bonding Motif Involving NH bonds of Ammonium Salts
and Macrocycles Derived from Platinum Corners and Butadiynediyl Linkers

Brenna K. Collins, Nattamai Bhuvanesh, and John A. Gladysz*

^aDepartment of Chemistry, Texas A&M University, PO Box 30012, College Station, Texas

77842-3012, USA E-mail: gladysz@mail.chem.tamu.edu

Experimental

General. Reactions were carried out under inert atmospheres and workups were conducted in air. Most instrumental procedures and chemical sources were detailed in a previous paper.^{s1} The following were new to this study and used as received: HNEt₂ (99+%, Alfa Aesar), NEt₃ (>99+%, EMD), Diallylamine (99%, Sigma Aldrich), Morpholine (99%, Alfa Aesar), KI (>99%, Baker). The cryoprobe ¹³C{¹H} NMR and ESI and APCI mass spectra were recorded using 500 MHz Bruker Avance and Thermo Scientific Q Exactive Focus instruments.

(Me₂C(CH₂PPh₂)₂)PtCl₂.^{s1,s2} A Schlenk flask was charged with (THT)₂PtCl₂ (1.0196 g, 2.3051 mmol), Me₂C(CH₂PPh₂)₂ (1.22 g, 2.766 mmol), and CH₂Cl₂ (20 mL) with stirring. After 24 h, the solvent was removed by rotary evaporation. The residue was washed with Et₂O (150 mL), H₂O (100 mL), and hexanes (100 mL), and dried by oil pump vacuum to give the product as a white solid (1.5644 g, 2.2143 mmol, 96%).

(Et₂C(CH₂PPh₂)₂)PtCl₂.^{s1,s2} A Schlenk flask was charged with (THT)₂PtCl₂ (0.5000 g, 1.1304 mmol), Et₂C(CH₂PPh₂)₂ (0.583 g, 1.243 mmol), and CH₂Cl₂ (20 mL) with stirring. After 24 h, the solvent was removed by rotary evaporation. The residue was washed with Et₂O (150 mL), H₂O (100 mL), and hexanes (150 mL), and dried by oil pump vacuum to give the product as a white solid (0.798 g, 1.086 mmol, 96%).

(Me₂C(CH₂PPh₂)₂)PtI₂. A round-bottom flask was charged with (Me₂C(CH₂PPh₂)₂)PtCl₂ (0.1004 g, 0.1421 mmol), KI (0.0795 g, 0.4789 mmol), and CH₂Cl₂ (15 mL) with stirring. After 48 h, the solvent was removed by rotary evaporation. The residue was washed with H₂O (3 x 30 mL) and Et₂O (3 x 30 mL) and dried by oil pump vacuum (3 h) to give (Me₂C(CH₂PPh₂)₂)PtI₂ as a bright yellow solid (0.1138 g, 0.1280 mmol, 90%) that darkened at 370 °C and blackened at 397 °C. Anal. Calcd. for C₂₉H₃₀I₂P₂Pt (889.40): C, 39.16; H, 3.40; Found: C, 40.98; H, 3.55.

NMR (δ (ppm), CD₂Cl₂): ¹H (500 MHz) 7.96-7.89 (m, 8H, *m* to P), 7.54-7.49 (m, 12H, *m* and *p* to P), 2.37 (d, ²J_{HP} = 9.5 Hz, 4H, PCH₂), 0.52 (s, 6H, CH₃); ¹³C{¹H} ^{s3} 135.0 (virtual t, ^{s4} ²J_{CP} = 4.7 Hz, *o* to P), 132.0 (m *J* = 72.5 Hz, *J* = 4.7 Hz, *i* to P), 131.6 (s, *p* to P), 128.6 (virtual t, ^{s4} ³J_{CP} = 5.8 Hz, *m* to P), 35.5 (t, ¹J_{CP} = 21.8 Hz, PCH₂), 32.4 (t, ²J_{CP} = 7.2 Hz, C(CH₂)₄), 30.4

($\underline{\text{C}}\text{H}_3$); $^3\text{P}\{^1\text{H}\} -6.2$ (s, $^1J_{\text{PPt}} = 3223$ Hz).^{s5}

IR (cm^{-1} , powder film): 2895 (m), 1435 (s), 1099 (s), 841 (s), 802 (s), 746 (s). MS:^{s7} ESI⁺, 762.0497 ($[\text{M} - \text{I}]^+$ (calc. 762.0510), 100%).

(Et₂C(CH₂PPh₂)₂)PtI₂. A round-bottom flask was charged with (Et₂C(CH₂PPh₂)₂)PtCl₂ (0.1030 g, 0.1402 mmol), KI (0.0710 g, 0.4277 mmol), CH₂Cl₂ (10 mL), and acetone (10 mL) with stirring. After 24 h, the solvent was removed by rotary evaporation. The residue was washed with H₂O (3 x 30 mL) and Et₂O (3 x 30 mL) and dried by oil pump vacuum (3 h) to give (Et₂C(CH₂PPh₂)₂)PtI₂ as a yellow solid (0.1237 mg, 0.1348 mmol, 96%) that blackened at 354 °C and further decomposed at 387 °C. Anal. Calcd. for C₃₁H₃₄I₂P₂Pt (917.45): C, 40.58; H, 3.74; Found: C, 41.16; H, 3.70.

NMR (δ (ppm), CD₂Cl₂): ^1H (500 MHz) 7.99-7.93 (m, 8H, *o* to P), 7.56-7.51 (m, 12H, *m* and *p* to P), 2.34 (d, $^2J_{\text{HP}} = 9.4$ Hz, 4H, P $\underline{\text{C}}\text{H}_2$), 0.89 (q, $^3J_{\text{HH}} = 7.4$ Hz, 4H, $\underline{\text{C}}\text{H}_2\text{CH}_3$), 0.26 (t, $^3J_{\text{HH}} = 7.4$ Hz, 6H, $\underline{\text{C}}\text{H}_3$); $^{13}\text{C}\{^1\text{H}\}$ ^{s3} 135.0 (virtual t, s4 $^2J_{\text{CP}} = 5.4$ Hz, *o* to P), 132.0 (m, $J = 70.4$ Hz, $J = 5.7$ Hz, *i* to P), 131.6 (s, *p* to P), 128.6 (virtual t, s4 $^3J_{\text{CP}} = 5.7$ Hz, *m* to P), 41.2 (s, $\underline{\text{C}}\text{H}_2\text{CH}_3$), 35.5 (t, $^1J_{\text{CP}} = 21.2$ Hz, P $\underline{\text{C}}\text{H}_2$), 32.4 (t, $^2J_{\text{CP}} = 8.1$ Hz, $\underline{\text{C}}(\text{CH}_2)_4$), 6.4 (s, $\underline{\text{C}}\text{H}_3$); $^3\text{P}\{^1\text{H}\} -7.0$ (s, $^1J_{\text{PPt}} = 3214$ Hz).^{s5}

IR (cm^{-1} , powder film): 2974 (w), 2914 (w), 2849 (w), 1437 (s), 1099 (s), 820 (m), 741 (s). MS:^{s7} ESI⁺, 790.0812 ($[\text{M} - \text{I}]^+$ (calc. 790.0823), 70%).

[(Me₂C(CH₂PPh₂)₂)Pt(C \equiv C)₂]₄·[H₂NEt₂⁺I⁻] (1·Ha⁺I⁻). A Schlenk flask was charged with (Me₂C(CH₂PPh₂)₂)PtI₂ (0.3652 g, 0.4106 mmol), (Me₂C(CH₂PPh₂)₂)Pt((C \equiv C)₂H)₂ (0.3007 g, 0.4098 mmol),^{s1} THF (150 mL), HNEt₂ (60 mL), and CuI (0.0186 g, 0.0977 mmol) with stirring and heated to 55 °C. After 3 d, the precipitate was isolated by filtration, washed with Et₂O (400 mL) and hexanes (400 mL), and dried by oil pump vacuum (rt, 20 h) to give 1·Ha⁺I⁻ as a bright yellow solid (0.4430 g, 0.1509 mmol, 74%) that blackened at 200 °C and further decomposed at 221 °C. ^1H and $^{13}\text{C}\{^1\text{H}\}$ NMR spectra showed minor impurities. Anal. Calcd. for C₁₃₆H₁₃₂INP₈Pt₄ (2935.59): C, 55.64; H, 4.53; N, 0.48; I, 4.32; Found: C, 50.55; H, 4.54; N, 0.50; I, 4.43.

NMR (δ (ppm), CD₂Cl₂): ^1H 7.64 (t, 32H, $^3J_{\text{HH}} = 8.8$ Hz, *m* to P), 7.29 (t, $^3J_{\text{HH}} = 7.8$ Hz,

16H, *p* to P), 7.17 (t, $^3J_{\text{HH}} = 8.0$ Hz, 32H, *o* to P), 3.51 (br s, 4H, NCH₂), 2.27 (d, $^2J_{\text{HP}} = 9.9$ Hz, 16H, PCH₂), 1.35 (t, $^3J_{\text{HH}} = 6.6$ Hz, 6H, NCH₂CH₃), 0.67 (s, 24H, CH₃); $^{13}\text{C}\{^1\text{H}\}$ 133.9 (virtual t, $^s4^2J_{\text{CP}} = 5.0$ Hz, *o* to P), 132.5 (m, $^s6^J = 66.3$ Hz, $J = 10.1$ Hz, *i* to P), 130.3 (s, *p* to P), 128.0 (virtual t, $^s4^3J_{\text{CP}} = 5.1$ Hz, *m* to P), 96.2 (m, PtC≡C), 93.1 (dd, $^2J_{\text{CP}} = 146.9$ Hz, $^2J_{\text{CP}} = 21.8$ Hz, PtC≡C), 44.9 (s, NCH₂), 37.2 (t, $^2J_{\text{CP}} = 16.6$ Hz, C(CH₂)₄), 35.9 (s, CH₃), 32.6 (t, $^1J_{\text{CP}} = 7.2$ Hz, PCH₂), 12.1 (s, NCH₂CH₃); $^{31}\text{P}\{^1\text{H}\}$ -5.6 (s, $^1J_{\text{PPt}} = 2217$ Hz).^{s5}

IR (cm⁻¹, powder film): 3051 (w), 2954 (m), 2864 (m), 2151 (w, $\nu_{\text{C}\equiv\text{C}}$), 1574 (m), 1433 (s), 1097 (s), 804 (s), 723 (s), 691 (s). MS:^{s7} ESI⁺, 1478.9111 ([M' + H₂NEt₂ + I + Na + H]²⁺ (calc. 1479.2938), 100%), 1404.3522 ([M' + H + H₂NEt₂]²⁺ (calc. 1404.3467), 81%), 1378.7930 ([M' + Na + H]²⁺ (calc. 1378.7931), 25%); MALDI⁺ (matrix DCTB), 2733 ([M' + H]⁺, 100%).

[(Me₂C(CH₂PPh₂)₂)Pt(C≡C)₂]₄·[H₂N(CH₂CH₂)₂O⁺I⁻]₃ (1·(Hc⁺I⁻)₃). A Schlenk flask was charged with (Me₂C(CH₂PPh₂)₂)PtI₂ (0.1004 g, 0.1129 mmol), (Me₂C(CH₂PPh₂)₂)Pt((C≡C)₂H)₂ (0.0953 g, 0.1299 mmol), THF (50 mL), morpholine (25 mL), and CuI (0.008 g, 0.042 mmol) with stirring and heated to 60 °C. After 6 d, the yellow precipitate was isolated by filtration, washed with Et₂O (150 mL) and hexanes (150 mL). While on the frit, the sample was dissolved in CH₂Cl₂ and filtered into a fresh flask. The solvent was removed from the filtrate by rotary evaporation and dried by oil pump vacuum (rt, 20 h) to give 1·(Hc⁺I⁻)₃ as a yellow-orange solid (0.1208 g, 0.0357 mmol, 63%) that blackened at 133 °C and melted at 205 °C. Anal. Calcd. for C₁₄₄H₁₅₀I₃N₃O₃P₈Pt₄ (3379.64): C, 51.18; H, 4.47; N, 1.24; I, 11.26; Found: C, 51.70; H, 4.61; N, 1.67; I, 7.10.

NMR (δ (ppm), CDCl₃): ^1H 7.65 (t, 32H, $^3J_{\text{HH}} = 7.2$ Hz, *m* to P), 7.30 (t, $^3J_{\text{HH}} = 7.3$ Hz, 16H, *p* to P), 7.21 (t, $^3J_{\text{HH}} = 6.8$ Hz, 32H, *o* to P), 3.53 (br s, 12H, OCH₂), 2.94 (br s, 12H, NCH₂), 2.33 (d, $^2J_{\text{HP}} = 7.1$ Hz, 16H, PCH₂), 0.63 (s, 24H, CH₃); $^{13}\text{C}\{^1\text{H}\}$ 134.0 (s, *o* to P), 132.4 (m, $^s6^J = 65.2$ Hz, $J = 6.8$ Hz, *i* to P), 130.4 (s, *p* to P), 128.2 (virtual t, $^s4^3J_{\text{CP}} = 5.0$ Hz, *m* to P), 97.4 (m, PtC≡C), 93.1 (dd, $^2J_{\text{CP}} = 138.2$ Hz, $^2J_{\text{CP}} = 19.9$ Hz, PtC≡C), 66.1 (s, OCH₂), 44.9 (s, NCH₂), 37.4 (t, $^2J_{\text{CP}} = 16.0$ Hz, C(CH₂)₄), 36.1 (s, CH₃), 33.1 (t, $^1J_{\text{CP}} = 6.9$ Hz, PCH₂); $^{31}\text{P}\{^1\text{H}\}$ -5.3 (s, $^1J_{\text{PPt}} = 2220$ Hz).^{s5}

IR (cm⁻¹, powder film): 3049 (w), 2935 (m), 2924 (w), 2858 (w), 2156 (w, $\nu_{\text{C}\equiv\text{C}}$), 1645 (w), 1433 (s), 1097 (s), 804 (m), 723 (s). MS:^{s7} ESI⁺, 1411.3357 ([**M'** + H₂N(CH₂CH₂)₂O + H]²⁺ (calc. 1410.3320), 100%); MALDI⁺ (matrix DCTB), 2734 ([**M'** + H]⁺, 50%).

$[(\text{Et}_2\text{C}(\text{CH}_2\text{PPh}_2)_2)\text{Pt}(\text{C}\equiv\text{C})_2]_4 \cdot [\text{H}_2\text{NEt}_2^+\text{I}^-] (2 \cdot \text{Ha}^+\text{I}^-)$. A Schlenk flask was charged with (Et₂C(CH₂PPh₂)₂)PtI₂ (0.3627 g, 0.3953 mmol), (Et₂C(CH₂PPh₂)₂)Pt((C≡C)₂H)₂ (0.3002 g, 0.3941 mmol),^{s1} THF (150 mL), HNEt₂ (60 mL), and CuI (0.022 g, 0.116 mmol) with stirring and heated to 55 °C. After 3 d, the precipitate was isolated by filtration, washed with Et₂O (400 mL) and hexanes (400 mL), and dried by oil pump vacuum (rt, 20 h) to give **2**·Ha⁺I⁻ as a yellow solid (0.4347 g, 0.1426 mmol, 72%) that blackened at 207 °C and further decomposed at 250 °C. The ¹H and ¹³C{¹H} NMR spectra showed minor impurities.

NMR (δ (ppm), CD₂Cl₂): ¹H 7.66 (t, ³J_{HH} = 9.0 Hz, 32H *m* to P), 7.29 (t, ³J_{HH} = 7.4 Hz, 16H, *p* to P), 7.16 (t, ³J_{HH} = 7.4 Hz, 32H, *o* to P), 3.57 (br s, 4H, NCH₂), 2.26 (d, ²J_{HP} = 9.0 Hz, 16H, PCH₂), 1.37 (t, ³J_{HH} = 7.3 Hz, 6H, NCH₂CH₃), 1.10 (q, ³J_{HH} = 7.0 Hz, 16H, CH₂CH₃), 0.25 (t, ³J_{HH} = 7.3 Hz, 24H, CH₃); ¹³C{¹H} 134.2 (virtual t, ^{s4} ²J_{CP} = 4.9 Hz, *o* to P), 133.1 (m^{s6} *J* = 58.5 Hz, *J* = 8.8 Hz, *i* to P), 130.6 (s, *p* to P), 128.4 (virtual t, ^{s4} ³J_{CP} = 5.0 Hz, *m* to P), 96.4 (m, PtC≡C), 93.6 (dd, ²J_{CP} = 145.2 Hz, ²J_{CP} = 20.5 Hz, PtC≡C), 45.4 (s, NCH₂), 41.9 (s, CH₂CH₃), 34.1 (t, ¹J_{CP} = 17.2 Hz, PCH₂), 32.5 (t, ²J_{CP} = 7.1 Hz, C(CH₂)₄), 12.5 (s, NCH₂CH₃), 6.7 (s, CH₃); ³¹P{¹H} -7.2 (s, ¹J_{Ppt} = 2222 Hz).^{s5} MS:^{s7} ESI⁺, 1460.9137 ([**M'** + H₂NEt₂ + H]²⁺ (calc. 1460.4093), 100%), 1432.3821 ([**M'** + H₃O + H]²⁺ (calc. 1432.8700), 63%); MALDI⁺ (matrix DCTB), 2846 ([**M'** + H]⁺, 100%).

$[(\text{Et}_2\text{C}(\text{CH}_2\text{PPh}_2)_2)\text{Pt}(\text{C}\equiv\text{C})_2]_4 \cdot [\text{H}_2\text{N}(\text{CH}_2\text{CH}=\text{CH}_2)_2^+\text{I}^-]_2 (2 \cdot \text{Hb}^+\text{I}^-)$. A Schlenk flask was charged with (Et₂C(CH₂PPh₂)₂)PtI₂ (0.0504 g, 0.0549 mmol), (Et₂C(CH₂PPh₂)₂)Pt((C≡C)₂-H)₂ (0.0502 g, 0.0659 mmol), THF (20 mL), diallylamine (10 mL), and CuI (0.0033 g, 0.0173 mmol) with stirring and heated to 60 °C. After 3 d, the precipitate was isolated by filtration, washed with Et₂O (100 mL) and hexanes (100 mL), and dried by oil pump vacuum (rt, 8 h) to give **2**·Hb⁺I⁻ as a bright yellow solid (0.0352 g, 0.0115 mmol, 42%) that blackened at 180 °C and further decomposed at 242 °C. Anal. Calcd. for C₁₄₆H₁₄₉INP₈Pt₄ (3072.84): C, 57.07; H, 4.89; N, 0.46; I, 4.13;

Found: C, 55.00; H, 4.86; N, 0.64; I, 4.30.

NMR (δ (ppm), CDCl_3): ^1H 7.68 (t, $^3J_{\text{HH}} = 8.8$ Hz, 32H, *m* to P), 7.21 (t, $^3J_{\text{HH}} = 7.6$ Hz, 16H, *p* to P), 7.05 (t, $^3J_{\text{HH}} = 7.3$ Hz, 32H, *o* to P), 6.27 (m with fine structure, 2H, $\text{NCH}_2\text{CH=}$), 5.86 (d, $^3J_{\text{HHtrans}} = 17.8$ Hz, 2H, $\text{NCH}_2\text{CH=CH}_E\text{H}_Z$), 5.42 (d, $^3J_{\text{HHcis}} = 11.5$ Hz, 2H, $\text{NCH}_2\text{CH=CH}_E\text{H}_Z$), 4.43 (apparent d, $^2J_{\text{HH}} = 6.4$ Hz, 4H, $\text{NCH}_2\text{CH=}$), 2.21 (d, $^2J_{\text{HP}} = 8.9$ Hz, 16H, PCH_2), 1.10 (q, $^3J_{\text{HH}} = 7.2$ Hz, 16H, CH_2CH_3), 0.23 (t, $^3J_{\text{HH}} = 7.3$ Hz, 24H, CH_3); $^{13}\text{C}\{^1\text{H}\}$ 134.2 (virtual t, $^s4^2J_{\text{CP}} = 5.0$ Hz, *o* to P), 133.0 (m, $^s6J = 57.8$ Hz, $J = 8.4$ Hz, *i* to P), 130.2 (s, *p* to P), 129.2 (s, $\text{NCH}_2\text{CHCH}_2$), 128.2 (virtual t, $^s4^3J_{\text{CP}} = 4.7$ Hz, *m* to P), 123.3 (s, $\text{NCH}_2\text{CHCH}_2$), 97.2 (m with t component, $J = 20.2$ Hz, $\text{PtC}\equiv\text{C}$), 92.2 (dd, $^2J_{\text{CP}} = 149.8$ Hz, $^2J_{\text{CP}} = 21.7$ Hz, $\text{PtC}\equiv\text{C}$), 51.8 (s, $\text{NCH}_2\text{CHCH}_2$), 41.6 (s, CH_2CH_3), 34.5 (t, $^1J_{\text{CP}} = 17.6$ Hz, PCH_2), 32.2 (t, $^2J_{\text{CP}} = 5.7$ Hz, $\text{C}(\text{CH}_2)_4$), 6.7 (s, CH_3); $^{31}\text{P}\{^1\text{H}\}$ -7.76 (s, $^1J_{\text{PPt}} = 2228$ Hz).^{s5}

IR (cm^{-1} , powder film): 3061 (m), 2939 (m), 2924 (m), 2856 (m), 2147 (w, $\nu_{\text{C}\equiv\text{C}}$), 1616 (w), 1433 (s), 1097 (s), 740 (s), 661 (s). MS:^{s7} ESI^+ , 1455.3251 ($[\text{M}' + \text{Cu} + \text{H}]^{2+}$ (calc. 1454.8256), 55%), 1432.3777 ($[\text{M}' + \text{H} + \text{H}_3\text{O}]^{2+}$ (calc. 1432.8700), 100%); APCI^+ , 2944.6357 ($[\text{M}' + \text{H}_2\text{N}(\text{CH}_2\text{CH}=\text{CH}_2)_2]^{+}$ (calc. 2943.8176), 1%, 10% for ions of $m/z > 1650$), 2910.6572 ($[\text{M}' + \text{Cu}]^{+}$ (calc. 2909.6517), 12%, 100% for ions of $m/z > 1650$).

$[(\text{Et}_2\text{C}(\text{CH}_2\text{PPh}_2)_2)\text{Pt}(\text{C}\equiv\text{C})_2]_4 \cdot [\text{HNEt}_3^+\text{I}^-]_3 \cdot (2 \cdot (\text{Hd}^+\text{I}^-))_3$. A Schlenk flask was charged with $(\text{Et}_2\text{C}(\text{CH}_2\text{PPh}_2)_2)\text{PtI}_2$ (0.1003 g, 0.1093 mmol), $(\text{Et}_2\text{C}(\text{CH}_2\text{PPh}_2)_2)\text{Pt}((\text{C}\equiv\text{C})_2\text{H})_2$ (0.1001 g, 0.1314 mmol), THF (50 mL), NEt_3 (20 mL), and CuI (0.0067 g, 0.0352 mmol) with stirring and heated to 60 °C. After 4 d, the precipitate was isolated by filtration, washed with Et_2O (300 mL) and hexanes (300 mL), and dried by oil pump vacuum (rt, 20 h) to give $2 \cdot (\text{Hd}^+\text{I}^-)_3$ as a yellow solid (0.1777 g, 0.0503 mmol, 92%) that blackened at 199 °C and further decomposed at 220 °C. Anal. Calcd. for $\text{C}_{158}\text{H}_{184}\text{I}_3\text{N}_3\text{P}_8\text{Pt}_4$ (3534.07): C, 53.70; H, 5.25; N, 1.19; I, 10.77; Found: C, 51.38; H, 5.01; N, 1.18; I, 11.24.

NMR (δ (ppm), CD_2Cl_2): ^1H 7.65 (t, $^3J_{\text{HH}} = 8.3$ Hz, 32H, *m* to P), 7.29 (t, $^3J_{\text{HH}} = 7.3$ Hz, 16H, *p* to P), 7.16 (t, $^3J_{\text{HH}} = 7.3$ Hz, 32H, *o* to P), 3.01 (q, $^3J_{\text{HH}} = 7.2$ Hz, 18H, NCH_2), 2.27 (d, $^2J_{\text{HP}} = 9.4$ Hz, 16H, PCH_2), 1.19 (t, $^3J_{\text{HH}} = 7.3$ Hz, 27H, NCH_2CH_3), 1.08 (q, $^3J_{\text{HH}} = 6.5$ Hz,

16H, $\underline{CH}_2\text{CH}_3$), 0.23 (t, $^3J_{\text{HH}} = 6.9$ Hz, 24H, \underline{CH}_3); $^{13}\text{C}\{^1\text{H}\}$ 134.5 (virtual t, s4 $^2J_{\text{CP}} = 5.0$ Hz, *o* to P), 133.1 (m, s6 $J = 58.6$ Hz, $J = 8.1$ Hz, *i* to P), 130.5 (s, *p* to P), 128.4 (s, *m* to P), 97.0 (m, PtC \equiv C), 92.4 (dd, $^2J_{\text{CP}} = 152.5$ Hz, $^2J_{\text{CP}} = 17.7$ Hz, PtC \equiv C), 46.9 (s, N \underline{CH}_2), 41.9 (s, $\underline{CH}_2\text{CH}_3$), 34.1 (t, $^1J_{\text{CP}} = 18.1$ Hz, P \underline{CH}_2), 32.4 (t, $^2J_{\text{CP}} = 5.8$ Hz, $\underline{C}(\text{CH}_2)_4$), 9.1 (s, N $\underline{CH}_2\text{CH}_3$), 6.6 (s, \underline{CH}_3); $^{31}\text{P}\{^1\text{H}\} -7.0$ (s, $^1J_{\text{PPt}} = 2204$ Hz).^{s5}

IR (cm^{-1} , powder film): 3049 (w), 2963 (w), 2935 (w), 2878 (w), 2142 (w, $\nu_{\text{C}\equiv\text{C}}$) 1433 (s), 1120 (m), 1098 (s), 831 (m), 740 (s). MS:^{s7} APCI⁺, 2946.6341 ($[\text{M}' + \text{HNET}_3]^+$ (calc. 2946.8411), 5%, 11% for ions of $m/z > 1500$), 2846.7391 ($[\text{M}' + \text{H}]^+$ (calc. 2846.7535), 45%, 100% for ions of $m/z > 1500$); MALDI⁺ (matrix DCTB), 2846 ($[\text{M}' + \text{H}]^+$, 100%).

DOSY NMR. Spectra were recorded on a Varian NMRS 500 MHz spectrometer equipped with a 5 mm Auto-Switchable probe and a *z* gradient coil (up to 30 G/cm). The probe temperature was kept at 25 °C, and the samples were allowed to equilibrate for at least 15 min. ^1H diffusion experiments were carried out with static samples using the convection-compensated bipolar pulse pair stimulated echo pulse sequence (Dbppste_cc).^{s8} The 90° pulse was 14.2 μs . The incremented gradient strength (*g*) was varied from 1 to 30 G/cm. The bipolar pulse gradient duration (δ) was 2 ms, and the diffusion period (Δ) was 30-50 ms. The number of transients per increment was 16 with a relaxation delay of 2 s. The field gradient strength was calibrated by measuring the self-diffusivity (*D*s) of 10% D₂O in H₂O ($D_s = 22.7 \times 10^{-1} \text{ m}^2 \text{ s}^{-1}$).^{s9} DOSY spectra were generated with the program MestReNova 6.0.2.^{s10}

Crystallography

A.^{s11} A CH_2Cl_2 solution of $\mathbf{1} \cdot \text{Ha}^+\text{I}^-$ was layered with hexanes. After 24 h, yellow blocks were obtained. The crystals were very unstable when removed from the mother liquor (presumed desolvation, including after mounting using various oils), complicating data collection, which is outlined in Table s1. Both Cu and Mo sources were used in efforts to optimize the data. Integrated intensity information for each reflection was obtained by reduction of the data frames with the program APEX3.^{s12} Lorentz, polarization, crystal decay, and absorption corrections were applied, the last with the program SADABS.^{s13} Some disordered dichloromethane molecules were found,

with partial occupancy per the formula unit $1 \cdot \text{Ha}^+ \text{I}^- \cdot 1.62 \text{CH}_2\text{Cl}_2$.^{s14-s16} Hydrogen atoms were placed in idealized positions using a riding model. All non-hydrogen atoms were refined with anisotropic thermal parameters. Appropriate restraints were added to keep the bond distances, angles, and thermal ellipsoids of the solvent molecules meaningful.^{s17} The absence of additional symmetry were confirmed using PLATON (ADDSYM).^{s18} The structure was refined (weighted least squares refinement on F^2) to convergence.^{s19,s20,s21}

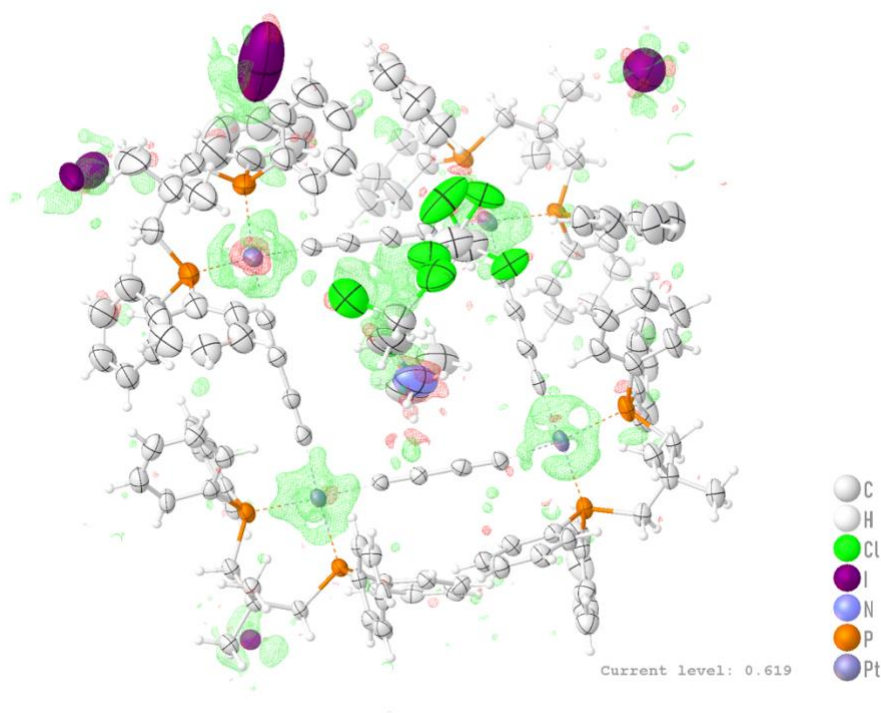


Figure s1. Residual electron density map for $1 \cdot \text{Ha}^+ \text{I}^-$ (see the `_refine_special_details` and/or `_vrf` responses to the CHECKCIF alerts in the CIF files for more details regarding the peaks).

B.^{s11} A CH_2Cl_2 solution of $1 \cdot \text{Hc}^+ \text{I}^-$ was layered with hexanes. After 24 h, yellow blocks were obtained that proved to be the anion metathesis product $1 \cdot \text{Hc}^+ \text{Cl}^-$, which were very unstable when removed from the mother liquor (presumed desolvation, including after mounting using various oils or in sealed glass capillaries). Data were collected as outlined in Table s1. Both Cu and Mo sources were used in efforts to optimize the data. Integrated intensity information for each reflection was obtained by reduction of the data frames with the program APEX3.^{s12} Lorentz, polarization, crystal decay, and absorption corrections were applied, the last with the program

SADABS.^{s13} Hydrogen atoms were placed in idealized positions using a riding model. All non-hydrogen atoms were refined with anisotropic thermal parameters. The absence of additional symmetry or voids were confirmed using PLATON (ADDSYM).^{s18} The morpholinium ion was modeled with the cyclohexane template in OLEX2 and was strongly restrained to keep the bond distances, angles, and thermal ellipsoids meaningful. The solvent molecules, all of which were disordered or in partially occupied positions, were MASKED with OLEX2. The structure was refined (weighted least squares refinement on F^2) to convergence.^{s19,s20} As noted in the text, the morpholine nitrogen atom has been reassigned from that in the CIF file to the atom that gives the closest H_2N interactions with the Pt_4C_{16} moiety.^{s22}

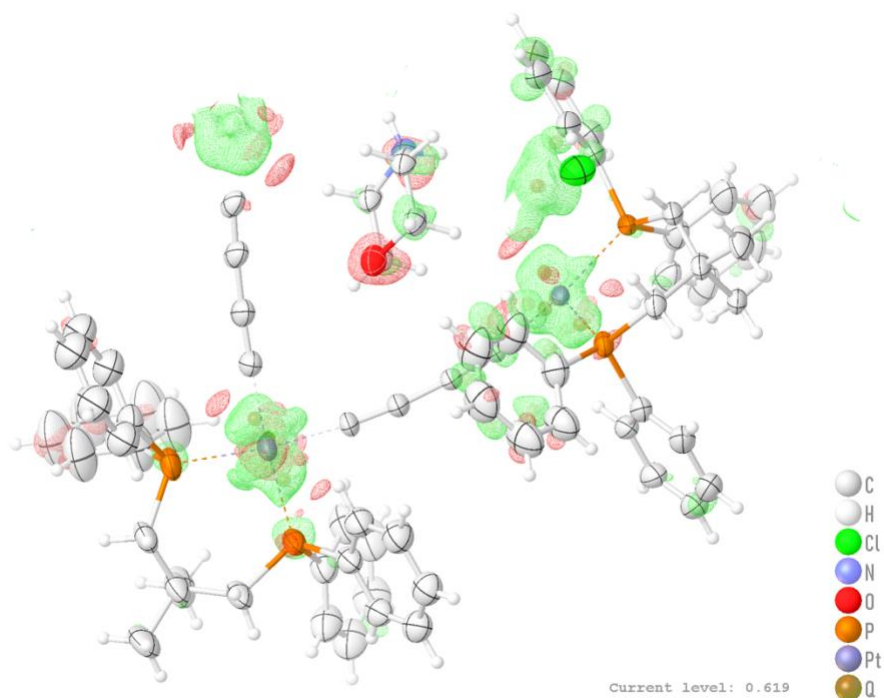


Figure s2. Residual electron density map for $1 \cdot (Hc^+Cl^-)_3$. (see the `_refine_special_details` and/or `_vrf` responses to the CHECKCIF alerts in the CIF files for more details regarding the peaks).

C.^{s11} A $CHCl_3$ solution of $2 \cdot Hb^+I^-$ was layered with toluene. After 24 h, colorless blocks were obtained. The crystals (including those grown from other solvent mixtures) were very unstable when removed from the mother liquor (presumed desolvation, including after mounting using various oils), complicating data collection, which is outlined in Table s1. Integrated intensity infor-

mation for each reflection was obtained by reduction of the data frames with the program APEX3.^{s12} Lorentz, polarization, crystal decay, and absorption corrections were applied, the last with the program SADABS.^{s13} A solution was readily obtained using XT/XS in APEX3.^{s12,s19} Hydrogen atoms were placed in idealized positions using a riding model. All non-hydrogen atoms were refined with anisotropic thermal parameters. The absence of additional symmetry and voids were confirmed using PLATON (ADDSYM).^{s18} Some disordered chloroform and toluene molecules were found, with partial occupancy per the formula unit $2 \cdot \text{Hb}^+\text{T}^- \cdot 3.75\text{CHCl}_3 \cdot 2.83\text{C}_7\text{H}_8$. Other residual electron density peaks could not be modeled, and were SQUEEZED using PLATON. Elongated ellipsoids on some of the phenyl groups indicated possible disorder, but no further modeling efforts were undertaken. The structure was refined (weighted least squares refinement on F^2) to convergence.^{s19,s20,s23}

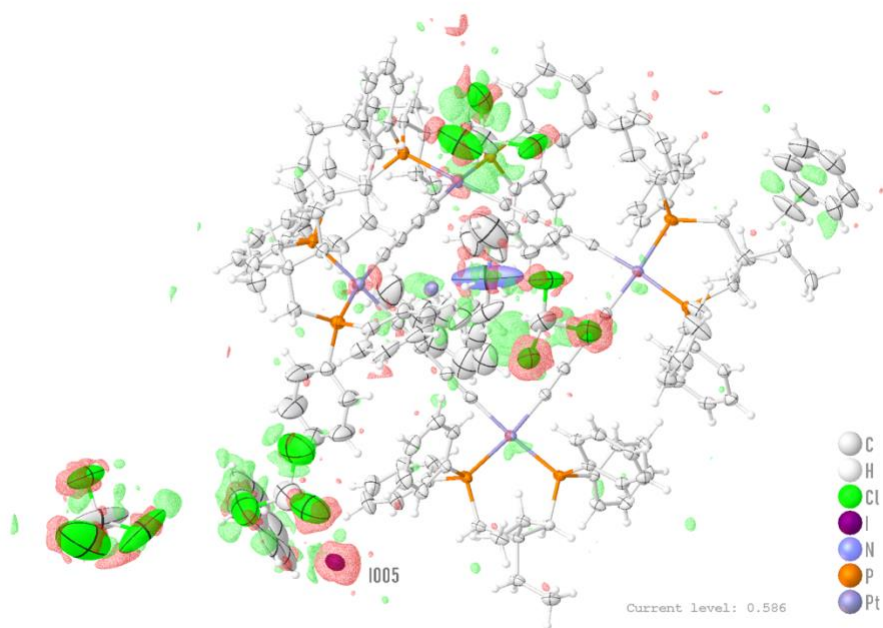


Figure s3. Residual electron density map for $2 \cdot \text{Hb}^+\text{T}^-$ (see the `_refine_special_details` and/or `_vrf` responses to the CHECKCIF alerts in the CIF files for more details regarding the peaks).

References

(s1) Collins, B. K.; Clough-Mastry, M.; Ehnbohm, A.; Bhuvanesh, N.; Hall, M. B.; Gladysz, J. A. Macrocyclic Complexes Derived from Four *cis*-L₂Pt Corners and Four Butadiynediyl Linkers; Syntheses, Electronic Structures, and Square versus Skew Rhombus Geometries. *Chem. Eur. J.* **2021**, *27*, 10021-10039.

(s2) van Rijn, J. A.; Siegler, M. A.; Spek, A. L.; Bouwman, E.; Drent, E. Ruthenium-Di-phosphine-Catalyzed Allylation of Phenols: A *gem*-Dialkyl-Type Effect Induces High Selectivity toward O-Allylation. *Organometallics*, **2009**, *28*, 7006-7014.

(s3) Due to the analyte solubility, this spectrum was recorded using a cryoprobe.

(s4) Hersh, W. H. False AA'X Spin-Spin Coupling Systems in ¹³C NMR: Examples Involving Phosphorous and a 20-Year-Old Mystery in Off-Resonance Decoupling. *J. Chem. Educ.* **1997**, *74*, 1485-1488.

(s5) This coupling represents a satellite (d, ¹⁹⁵Pt = 33.8%), and is not reflected in the peak multiplicity given.

(s6) This signal is part of a complex spin system^{s1} and the *J* values refer to a component that is an apparent dd.

(s7) *m/z*; **M'** refers to the mass of the neutral [L₂PtC₄]₄ macrocycle.

(s8) Jerschow, A.; Muller, N. Suppression of Convection Artifacts in Stimulated-Echo Diffusion Experiments. Double-Stimulated-Echo Experiments. *J. Magn. Reson.* **1997**, *125*, 372-375.

(s9) Antalek, B. Using pulsed gradient spin echo NMR for chemical mixture analysis: how to obtain optimum results. *Concepts Magn. Reson.* **2002**, *14*, 225-258.

(s10) *MestReNova*, version 6.0.2; Mestrelab Research: Santiago de Compostela, Spain, 2009.

(s11) For additional details on the challenges in solving this structure, see the checkCIF report.

(s12) APEX3 "Program for Data Collection on Area Detectors" BRUKER AXS Inc., 5465 East Cheryl Parkway, Madison, WI 53711-5373 USA.

(s13) SADABS, Sheldrick, G. M. "Program for Absorption Correction of Area Detector Frames", BRUKER AXS Inc., 5465 East Cheryl Parkway, Madison, WI 53711-5373 USA.

(s14) Only one iodide ion location could be found, occupying a special position (1/3,2/3, 0.199) with an occupancy of 0.3333. Since experimental data strongly suggested a full equivalent, iodide ions were distributed at the residual electron density peaks with restraints to ensure an overall occupancy of 1.

(s15) Fourier difference maps showed residual electron density peaks near the iodide ion locations, suggesting additional solvent molecules (disordered and/or with partial occupancies; R1 –5.81 and wR2 19.07 at this stage). Olex2 was used to mask these molecules (R1 –5.06 and wR2 14.81).

(s16) A solvent mask was calculated and 401 electrons were found in a volume of 4447 Å³ in 3 voids per unit cell. This is consistent with the presence of 1.5CH₂Cl₂ and 0.5H₂O per formula unit **1**·Ha⁺I⁻·1.62CH₂Cl₂, corresponding to 408 electrons per unit cell.

(s17) Some of the phenyl and methyl groups showed elongated ellipsoids suggesting possible disorder. Some of these were restrained with RIGU and SIMU. Residual electron density near the diethylammonium ion suggested minor disorder, but no effort was made to model this.

(s18) Spek, A. L. Single-crystal structure validation with the program *PLATON*. *J. Appl. Cryst.* **2003**, *36*, 7-13.; Spek, A. L., Utrecht University, Utrecht, The Netherlands **2008**.

(s19) (a) Sheldrick, G.M. A short history of SHELX. *Acta Crystallogr.* **2008**, *A64*, 112-122. (b) Sheldrick, G. M. *SHELXT* – Integrated space-group and crystal-structure determination. *Acta Crystallogr.* **2015**, *A71*, 3-8. (c) Sheldrick, G. M. Crystal structure refinement with *SHELXL*. *Acta Crystallogr.* **2015**, *C71*, 3-8.

(s20) Dolomanov, O. V.; Bourhis, L. J.; Gildea, R. J.; Howard, J. A. K.; Puschmann, H. OLEX2: a complete structure solution, refinement and analysis program, *J. Appl. Cryst.* **2009**, *42*, 339-341.

(s21) The following additional description was recommended by a reviewer. (a) Data were collected on several crystals from different preparative batches using both Cu and Mo sources (depending upon the quality and size of the crystals; the best structure model collected using Mo is reported). All the structure models indicate the presence of a diethylammonium cation occupying the void created by the Pt₄ core. However, it was clear that there was only one location for I (viz., I1), occupying special position (1/3,2/3,0.199), which accounts for an occupancy of 0.3333. The elemental analysis given with the synthesis confirms the presence of a full iodine (Calcd. I,

4.32; Found: I, 4.43). Thus, iodine has been distributed at some of the residual electron density peaks with a restraint setting the total occupancy to 1. The Fourier difference maps show several additional residual electron density peaks near the disordered iodine suggesting the presence of partially occupied and or disordered solvent. At this point the reliability factors were R_1 5.81 and wR_2 19.07. Olex2 was used to mask the latter solvent molecules, which decreased the reliability factors significantly R_1 5.06 and wR_2 14.81. No further experiments or checks were carried out to determine the exact location(s) of the iodine atoms. A solvent mask was calculated and 401 electrons were found in a volume of 4447 Å³ in 3 voids per unit cell. This is consistent with the presence of 1.5[CH₂Cl₂], 0.5[H₂O] per asymmetric unit which accounts for 408 electrons per unit cell. (b) Residual electron density near diethylammonium ion suggested minor disorder. No efforts to model this disorder. Some of the phenyl groups and the terminal methyl groups showed elongated ellipsoids suggesting possible disorder. Some of these were restrained with RIGU and SIMU. Others were left alone, but these efforts reached a point of diminishing returns.

(s22) The following additional description was recommended by a reviewer. (a) Crystals of this complex were extremely unstable. Over 20 series of syntheses and crystallizations were carried out. Also, we tried soaking the crystals in several types of oil by themselves, saturated with the mother liquor, and the crystals in the mother liquor themselves. The crystals consistently lost solvent as they were picked and mounted on the cryo-stream. We also tried mounting the crystals at temperatures from 250 K to 110 K. In most cases, the crystals cracked. At room temperature, the crystals crumbled within a few seconds. The crystal that provided the reported data luckily survived at 110 K. However, analysis showed elongated ellipsoids on most of the atoms, suggesting whole molecule disorder. Significant residual electron density (8.1) near one of the Pt atoms also supports the assignment of whole molecule disorder. Given only half the molecule forms the asymmetric unit and the symmetry of the space group, attempts to model the disorder required large numbers of restraints and constraints. In addition, the solvent molecules could not be located from the residual electron density maps. Further, the final results with the disorder modeled and solvent MASKED using OLEX2 did afford improvement. For our final refinement, strong restraints and constraints were used to keep all the thermal ellipsoids meaningful, assuming no disorder. We also MASKED the partially occupied and or disordered solvents with OLEX2. The morpholinium ion was modelled with a cyclohexane template in OLEX2 and was strongly restrained to keep the

bond distances, angles, and thermal ellipsoids meaningful. (b) Given the complex instability of the crystal outside the mother liquor, this was the best result we could extract out of the compound. Efforts to mount the crystals in sealed glass capillaries and collect the data was also not fruitful. (c) The reported data were collected on a Cu source. We have also tried collecting the data on a Mo source. The results were similar, but not any better.

(s23) The following additional description was recommended by a reviewer. (a) The crystal used was grown in layered CHCl_3 and toluene. Trials with many other solvent mixtures including CH_2Cl_2 and hexanes and other options produced crystals that were extremely unstable. In spite of trials using different oils as protectants, the crystals died as they were picked and mounted at 110 K. (b) Data were also collected at 250 K (suspecting a phase transition at lower temperature), but this did not help. In some of the crystals the diffraction quality worsened as the data were collected. This was attributed to solvent loss outside the mother liquor, even at 110 K. (c) A few rare crystals survived and the one used was one of the better in this series. Nonetheless, the data indicated significant disorder as well as partial solvent occupancy. (d) In addition, there were a few strong residual electron density peaks, which possibly indicate either residual starting material or product with partial loss of solvent coexisting in the structure. Whole molecule disorder remains another possibility. Although we have successfully located and modeled part of the solvents (chloroform and toluene, with elongated ellipsoids), some of the partially occupied and/or disordered solvent could not be located. These were SQUEEZED using PLATON. (e) Elongated ellipsoids on some of the terminal atoms possibly indicated disorder. No efforts were made to model this disorder. Similarly, elongated ellipsoids associated with the $n\text{-propyl})_2\text{N}^+$ moiety suggested disorder but this was not modeled in view of diminishing returns. (f) Strong residual electron densities were present at the locations assigned as Pt5 and Pt6 (dummy atoms with partial occupancies 0.11 and 0.03). Removing these atoms made the $(n\text{-propyl})_2\text{N}^+$ ion unstable, drifting towards the Pt5 and Pt6 locations. Pt5 and Pt6 are thought to be connected to factors noted above (residual reactant, product with partial solvent loss, whole molecule disorder, etc.). The $(n\text{-propyl})_2\text{N}^+$ moieties were not squeezed as they are part of the charge balance.

Table s1. General crystallographic data.

complex	$1 \cdot \text{Ha}^+\Gamma \cdot 1.62\text{CH}_2\text{Cl}_2^a$	$1 \cdot \text{Hc}^+\text{Cl}^-^a$	$2 \cdot \text{Hb}^+\Gamma \cdot (3.75\text{CHCl}_3)(2.83\text{C}_7\text{H}_8)^a$
empirical formula	$\text{C}_{137.62}\text{H}_{129.24}\text{Cl}_{3.24}\text{I}_{1.01}\text{NP}_8\text{Pt}_4$	$\text{C}_{136}\text{H}_{130}\text{Cl}\text{INOP}_8\text{Pt}_4$	$\text{C}_{169.56}\text{H}_{174.39}\text{Cl}_{11.25}\text{INP}_8\text{Pt}_{4.14}$
formula weight	3068.45	2857.97	3807.35
temperature [K]	110.0	110.0	110.0
diffractometer	Bruker QUEST	Bruker VENTURE	Bruker QUEST
wavelength [Å]	0.71073	1.54178	0.71073
crystal system	Trigonal	Monoclinic	Triclinic
space group	P-3	C2/c	P-1
unit cell dimensions:			
<i>a</i> [Å]	35.0101(8)	25.3077(14)	18.8201(16)
<i>b</i> [Å]	35.0101(8)	26.3723(14)	19.0800(15)
<i>c</i> [Å]	21.4586(5)	21.7373(12)	26.635(2)
α [°]	90	90	79.217(3)
β [°]	90	90.009(3)	76.791(3)
γ [°]	120	90	71.491(3)
<i>V</i> [Å ³]	22778.1(12)	14508.0(14)	8761.3(13)
<i>Z</i>	6	4	2
ρ_{calc} [Mg/m ³]	1.342	1.308	1.443
μ [mm ⁻¹]	4.061	8.372	3.762
F(000)	9016	5640	3772
crystal size [mm ³]	0.049 × 0.034 × 0.021	0.109 × 0.102 × 0.045	0.142 × 0.031 × 0.024
\varnothing limit [°]	1.777 to 25.019	2.420 to 70.258	1.749 to 27.508
index range (<i>h</i> , <i>k</i> , <i>l</i>)	-41, 41; -41, 41; -25, 25	-30, 30; -32, 32; -26, 26	-24, 24; -24, 24; -34, 34
reflections collected	528742	142334	492199
independent reflections	26831 [R(int) = 0.0807]	13825 [R(int) = 0.0646]	40243 [R(int) = 0.0683]
completeness to \varnothing	100.0	100.0	100.0
max. and min. transmission	0.4286 and 0.2722	0.3841 and 0.1542	0.1864 and 0.1313
data/restraints/parameters	26831 / 336 / 1445	13825 / 1084 / 620	40243 / 244 / 1773
goodness-of-fit on F ²	1.049	1.052	1.109
<i>R</i> indices (final) [<i>I</i> > 2 σ (<i>I</i>)]	$R_1 = 0.0506$, $wR_1 = 0.1286$	$R_1 = 0.0615$, $wR_1 = 0.1677$	$R_1 = 0.0398$, $wR_1 = 0.1138$
<i>R</i> indices (all data)	$R_2 = 0.0732$, $wR_2 = 0.1481$	$R_2 = 0.0640$, $wR_2 = 0.1703$	$R_2 = 0.0552$, $wR_2 = 0.1190$
largest diff. peak and hole [eÅ ⁻³]	2.107 and -1.103	8.094 and -2.333	4.522 and -1.690

^aFor all three salts, additional solvate molecules were present that were MASKED or SQUEEZED (see experimental section). Thus, the empirical formulae are misleading and some densities may be underestimated.

Table s2. Key crystallographic distances [Å] and angles [°] for Pt₄C₁₆ complexes.

	1·Ha⁺Γ⁻·1.62CH₂Cl₂	1·Hc⁺Cl⁻	2·Hb⁺I⁻·(3.75CHCl₃)(2.83C₇H₈)
Pt1-C1	2.006(8)	2.002(8)	2.019(5)
Pt1-C16	2.006(8)	1.992(6)	2.004(5)
Pt2-C4	1.991(9)	1.997(8)	2.006(5)
Pt2-C5	1.985(9)	1.990(7)	2.008(5)
Pt3-C8	2.017(8)	1.992(6)	2.003(5)
Pt3-C9	2.005(7)	2.002(8)	1.998(5)
Pt4-C12	1.994(7)	1.997(8)	2.010(5)
Pt4-C13	2.030(9)	1.990(7)	2.007(5)
Avg Pt-C	2.004(14) ^a	1.996(4)	2.007(6)
Pt1-P1	2.284(2)	2.275(18)	2.273(13)
Pt1-P2	2.291(2)	2.271(17)	2.275(12)
Pt2-P3	2.277(3)	2.272(19)	2.278(13)
Pt2-P4	2.273(3)	2.277(2)	2.276(13)
Pt3-P5	2.283(19)	2.275(18)	2.283(12)
Pt3-P6	2.281(2)	2.271(17)	2.284(12)
Pt4-P7	2.289(2)	2.272(19)	2.281(12)
Pt4-P8	2.270(2)	2.277(2)	2.289(12)
Avg Pt-P	2.281(7) ^a	2.274(2)	2.280(5)
C1≡C2	1.210(12)	1.208(11)	1.203(7)
C2-C3	1.391(13)	1.384(11)	1.378(7)
C3≡C4	1.202(12)	1.205(12)	1.205(7)
C5≡C6	1.214(12)	1.221(10)	1.199(7)
C6-C7	1.391(12)	1.373(10)	1.399(7)
C7≡C8	1.190(11)	1.205(9)	1.208(7)
C9≡C10	1.211(10)	1.208(11)	1.215(7)
C10-C11	1.371(11)	1.384(11)	1.381(7)
C11≡C12	1.217(11)	1.205(12)	1.206(7)
C13≡C14	1.194(12)	1.221(10)	1.202(7)
C14-C15	1.194(12)	1.373(10)	1.373(7)
C15≡C16	1.195(12)	1.205(9)	1.208(7)
Avg C≡C	1.204(10) ^a	1.210(7)	1.206(5)
C16-Pt1-C1	87.9(3)	87.1(3)	85.7(2)
C4-Pt2-C5	86.2(3)	85.2(3)	87.0(2)
C8-Pt3-C9	89.7(3)	87.1(3)	88.2(19)
C12-Pt4-C13	85.9(3)	85.2(3)	86.2(19)

Table s2. (Continued)

	1·Ha⁺I⁻·1.62CH₂Cl₂	1·Hc⁺Cl⁻	2·Hb⁺I⁻·(3.75CHCl₃)(2.83C₇H₈)
Avg C-Pt-C	87.4(2) ^a	86.2(1)	86.8(1)
Pt1-C1-C2	177.2(8)	176.9(7)	174.4(5)
C1-C2-C3	178.5(9)	174.7(10)	177.1(6)
C2-C3-C4	179.4(12)	175.9(10)	178.7(6)
C3-C4-Pt2	175.5(8)	176.0(8)	178.5(5)
Pt2-C5-C6	174.3(8)	174.8(7)	173.8(5)
C5-C6-C7	177.0(10)	174.8(8)	179.8(7)
C6-C7-C8	177.7(10)	174.3(7)	178.4(5)
C7-C8-Pt3	170.6(8)	170.9(6)	172.3(4)
Pt3-C9-C10	175.3(7)	176.9(7)	179.7(5)
C9-C10-C11	178.2(8)	174.7(10)	178.5(5)
C10-C11-C12	178.8(9)	175.9(10)	178.3(6)
C11-C12-Pt4	171.6(7)	176.0(8)	175.6(4)
Pt4-C13-C14	174.8(8)	174.8(7)	174.4(5)
C13-C14-C15	177.8(11)	174.8(8)	175.5(6)
C14-C15-C16	177.8(9)	174.3(7)	176.8(6)
C15-C16-Pt1	178.4(8)	170.9(6)	178.6(5)
Pt4-Pt1-Pt2 vs. Pt2-Pt3-Pt4 ^b	144	96	135
Pt1-Pt2 ^c	7.797	7.748	7.803
Pt1-Pt4	7.782	7.676	7.762
Pt2-Pt3	7.757	7.676	7.799
Pt3-Pt4	7.784	7.748	7.807
Pt1-Pt3	10.318	8.735	10.505
Pt2-Pt4	11.154	9.961	10.653

^a This represents the standard deviation of the averaged values. ^b Plane/plane angle. ^c The atom numbers have not been changed from those in the CIF file. In all case Pt2-Pt4 represents the longest platinum-platinum distance, as opposed to Pt1-Pt3 in the previous publication.^{s1}

Table s3. Hydrogen bonding interactions: short NH and NCH contacts to Pt₄C₁₆ macrocycles (cutoff ≤ 4 Å; the NH protons are arbitrarily designated with upper case letters (A, B, C), and NCH protons with lower case letters (a, b, c, d).

NH...C _{sp}	NH...(C≡C) _{centroid}	NCH...C _{sp}	NCH...(C≡C) _{centroid}
1·Ha⁺I⁻·1.62CH₂Cl₂			
3.60 (HA/C7)	3.44 (HA/C7≡C8)	2.84 (Ha/C1)	2.61 (Ha/C1≡C2)
3.37 (HA/C8)		2.50 (Ha/C2)	
2.62 (HA/C9)	2.41 (HA/C9≡C10)	2.80 (Ha/C3)	3.13 (Ha/C3≡C4)
2.35 (HA/C10)		3.52 (Ha/C4)	
3.13 (HB/C11)	3.22 (HB/C11≡C12)	3.58 (Ha/C15)	3.49 (Ha/C15≡C16)
3.42 (HB/C12)		3.50 (Ha/C16)	
3.06 (HB/C13)	2.84 (HB/C13≡C14)	3.28 (Hb/C3)	3.14 (Hb/C3≡C4)
2.73 (HB/C14)		3.46 (Hb/C4)	
		3.13 (Hb/C5)	2.83 (Hb/C5≡C6)
		2.64 (Hb/C6)	
		2.68 (Hb/C7)	2.92 (Hb/C7≡C8)
		3.25 (Hb/C8)	
		3.58 (Hc/C7)	3.56 (Hc/C7≡C8)
		3.64 (Hc/C8)	
		3.48 (Hd/C9)	3.94 (Hd/C9≡C10)
		3.34 (Hd/C10)	
		3.65 (Hd/C11)	3.36 (Hd/C11≡C12)
		4.30 (Hd/C12)	
1·Hc⁺Cl⁻			
2.77 (HA/C15)	2.59 (HA/C15≡C16)	2.98 (Ha/C1)	2.85 (Ha/C1≡C2)
2.55 (HA/C16)		2.85 (Ha/C2)	
2.52 (HA/C1)	2.48 (HA/C1≡C2)	3.19 (Ha/C3)	3.46 (Ha/C3≡C4)
2.59 (HA/C2)		3.82 (Ha/C4)	
3.03 (HB/C3)	3.10 (HB/C3≡C4)	3.94 (Hb/C5)	3.62 (Hb/C5≡C6)
3.28 (HB/C4)		3.38 (Hb/C6)	
3.10 (HB/C5)	2.89 (HB/C5≡C6)	3.13 (Hb/C7)	3.17 (Hb/C7≡C8)
2.80 (HB/C6)		3.31 (Hb/C8)	
		2.77 (Hc/C7)	2.59 (Hc/C7≡C8)
		2.55 (Hc/C8)	
		2.52 (Hc/C9)	2.48 (Hc/C9≡C10)
		2.59 (Hc/C10)	
		3.03 (Hd/C11)	3.10 (Hd/C11≡C12)
		3.28 (Hd/C12)	
		3.10 (Hd/C13)	2.89 (Hd/C13≡C14)
		2.80 (Hd/C14)	
2·Hb⁺I⁻·(3.75CHCl₃)(2.83C₇H₈)			
3.51 (HA/C11)	3.68 (HA/C11≡C12)	3.36 (Ha/C1)	2.97 (Ha/C1≡C2)
3.93 (HA/C12)		2.67 (Ha/C2)	

Table s3. (Continued)

NH...C _{sp}	NH...(C≡C) _{centroid}	NCH...C _{sp}	NCH...(C≡C) _{centroid}
3.94 (HA/C13)	3.71 (HA/C13≡C14)	2.50 (Ha/C3)	2.66 (Ha/C3≡C4)
3.57 (HA/C14)		2.94 (Ha/C4)	
2.71 (HB/C15)	2.70 (HB/C15≡C16)	3.54 (Ha/C5)	3.46 (Ha/C5≡C6)
2.83 (HB/C16)		3.47 (Ha/C6)	
3.20 (HB/C1)	3.14 (HB/C1≡C2)	3.44 (Hb/C5)	3.10 (Hb/C5≡C6)
3.18 (HB/C2)		2.85 (Hb/C6)	
		2.72 (Hb/C7)	2.88 (Hb/C7≡C8)
		3.15 (Hb/C8)	
		3.74 (Hb/C9)	3.69 (Hb/C9≡C10)
		3.73 (Hb/C10)	
		3.97 (Hc/C1)	3.68 (Hc/C1≡C2)
		3.46 (Hc/C2)	
		3.41 (Hc/C3)	3.57 (Hc/C3≡C4)
		3.82 (Hc/C4)	

Table s4. Short N and NC contacts to Pt₄C₁₆ macrocycles (cutoff ≤ 4 Å; the NC carbons are arbitrarily designated with upper case letters A, B).

N \cdots C _{sp}	N \cdots (C \equiv C) _{centroid}	NC \cdots C _{sp}	NC \cdots (C \equiv C) _{centroid}
1·Ha⁺I⁻·1.62CH₂Cl₂			
3.94 (N/C7)	3.88 (N/C7 \equiv C8)	3.81 (CA/C1)	3.55 (CA/C1 \equiv C2)
3.91 (N/C8)		3.37 (CA/C2)	
3.48 (N/C9)	3.27 (N/C9 \equiv C10)	3.37 (CA/C3)	3.55 (CA/C3 \equiv C4)
3.17 (N/C10)		3.82 (CA/C4)	
3.31 (N/C11)	3.56 (N/C11 \equiv C12)	3.94 (CA/C5)	3.69 (CA/C5 \equiv C6)
3.89 (N/C12)		3.52 (CA/C6)	
3.95 (N/C13)	3.75 (N/C13 \equiv C14)	3.49 (CA/C7)	3.66 (CA/C7 \equiv C8)
3.64 (N/C14)		3.91 (CA/C8)	
		3.90 (CB/C9)	3.79 (CB/C9 \equiv C10)
		3.77 (CB/C10)	
1·Hc⁺Cl⁻			
3.43 (N/C1)	3.28 (N/C1 \equiv C2)	3.53 (CA/C1)	3.44 (CA/C1 \equiv C2)
3.25 (N/C2)		3.45 (CA/C2)	
3.44 (N/C3)	3.64 (N/C3 \equiv C4)	3.72 (CA/C3)	3.95 (CA/C3 \equiv C4)
3.93 (N/C4)		4.25 (CA/C4)	
3.91 (N/C5)	3.65 (N/C5 \equiv C6)	3.55 (CB/C7)	3.49 (CB/C7 \equiv C8)
3.48 (N/C6)		3.53 (CB/C8)	
3.43 (N/C7)	3.56 (N/C7 \equiv C8)	3.43 (CB/C9)	3.28 (CB/C9 \equiv C10)
3.78 (N/C8)		3.25 (CB/C10)	
		3.44 (CB/C11)	3.64 (CB/C11 \equiv C12)
		3.93 (CB/C12)	
2·Hb⁺I⁻·(3.75CHCl₃)(2.83C₇H₈)			
3.86 (N/C1)	3.68 (N/C1 \equiv C2)	4.04 (CA/C1)	3.75 (CA/C1 \equiv C2)
3.60 (N/C2)		3.54 (CA/C2)	
3.52 (N/C15)	3.58 (N/C15 \equiv C16)	3.49 (CA/C3)	3.64 (CA/C3 \equiv C4)
3.74 (N/C16)		3.88 (CA/C4)	
		3.97 (CA/C5)	3.75 (CA/C5 \equiv C6)
		3.61 (CA/C6)	
		3.67 (CA/C7)	3.86 (CA/C7 \equiv C8)
		4.12 (CA/C8)	
		4.06 (CB/C1)	3.89 (CB/C1 \equiv C2)
		3.80 (CB/C2)	

Table s5. Diffusion coefficients (D) derived from DOSY ^1H NMR experiments in CDCl_3 .

complex	CDCl_3		CD_2Cl_2	
	signal (ppm)	$D \times 10^{10} (\text{m}^2\text{s}^{-1})$	signal (ppm)	$D \times 10^{10} (\text{m}^2\text{s}^{-1})$
1·Ha⁺I⁻	7.63	4.05 ± 0.01	7.64	9.69 ± 0.09
	7.19	3.96 ± 0.01	7.29	10.16 ± 0.20
	7.04	3.99 ± 0.01	7.17	9.79 ± 0.17
	3.79	4.05 ± 0.04	–	–
	2.22	4.00 ± 0.01	2.27	9.51 ± 0.13
	1.57	4.00 ± 0.02	1.35	10.10 ± 0.09
	0.70	3.97 ± 0.01	0.67	9.57 ± 0.18
1·(Hc⁺I⁻)₃	7.65	4.33 ± 0.02	7.65	8.38 ± 0.10
	7.24	4.31 ± 0.02	7.30	8.45 ± 0.15
	7.08	4.23 ± 0.03	7.21	8.64 ± 0.14
	3.52	8.73 ± 0.04	3.53	17.19 ± 0.12
	2.95	8.83 ± 0.05	2.94	17.21 ± 0.08
	2.33	4.36 ± 0.02	2.33	8.52 ± 0.13
	0.62	4.29 ± 0.03	0.63	8.60 ± 0.14
2·Ha⁺I⁻	7.66	3.75 ± 0.01		
	7.19	3.76 ± 0.01		
	7.03	3.78 ± 0.01		
	3.82	3.76 ± 0.02		
	2.22	3.79 ± 0.01		
	1.61	3.79 ± 0.01		
	1.10	3.78 ± 0.01		
0.21	3.75 ± 0.02			
2·Hb⁺I⁻	7.68	4.07 ± 0.08		
	7.21	3.94 ± 0.10		
	7.05	4.02 ± 0.10		
	6.27	4.63 ± 0.09		
	5.86	4.75 ± 0.10		
	5.42	4.73 ± 0.10		
	4.43	4.76 ± 0.09		
	2.22	4.09 ± 0.08		
	1.10	4.02 ± 0.09		
0.22	4.10 ± 0.07			
2·(Hd⁺I⁻)₃	7.64	4.03 ± 0.02	7.65	8.06 ± 0.11
	7.24	4.06 ± 0.01	7.29	8.22 ± 0.15
	7.08	4.07 ± 0.01	7.16	8.14 ± 0.13
	3.05	7.40 ± 0.03	3.01	17.41 ± 0.11
	2.23	4.02 ± 0.01	2.27	8.00 ± 0.11
	1.19	7.32 ± 0.03	1.19	16.87 ± 0.16
	1.07	4.14 ± 0.02	1.08	8.17 ± 0.13
	0.20	4.01 ± 0.02	0.23	8.11 ± 0.11

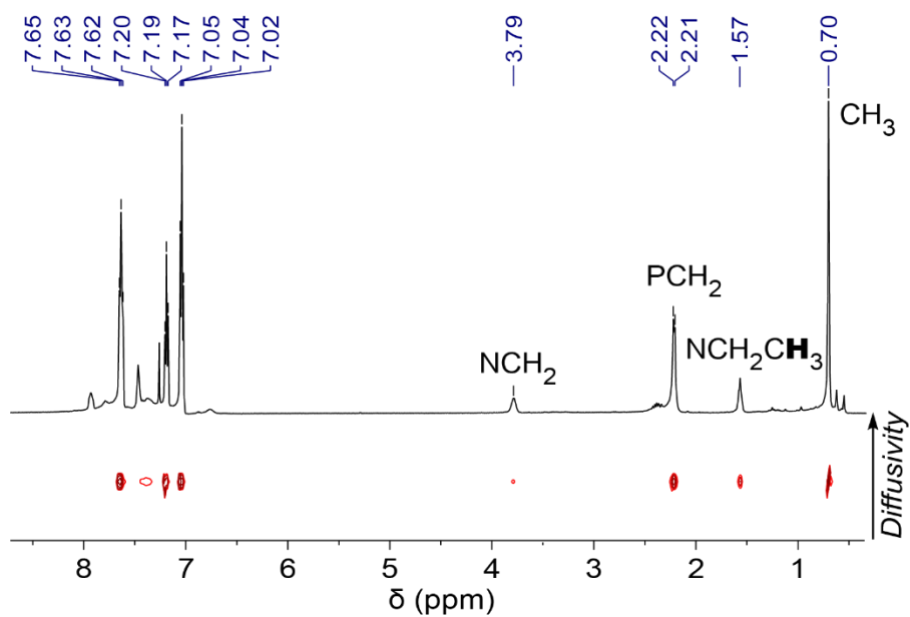


Figure s4. DOSY ^1H NMR plot (500 MHz, CDCl_3) of $1 \cdot \text{Ha}^+\text{I}^-$ (full version, Figure 3 in main text).

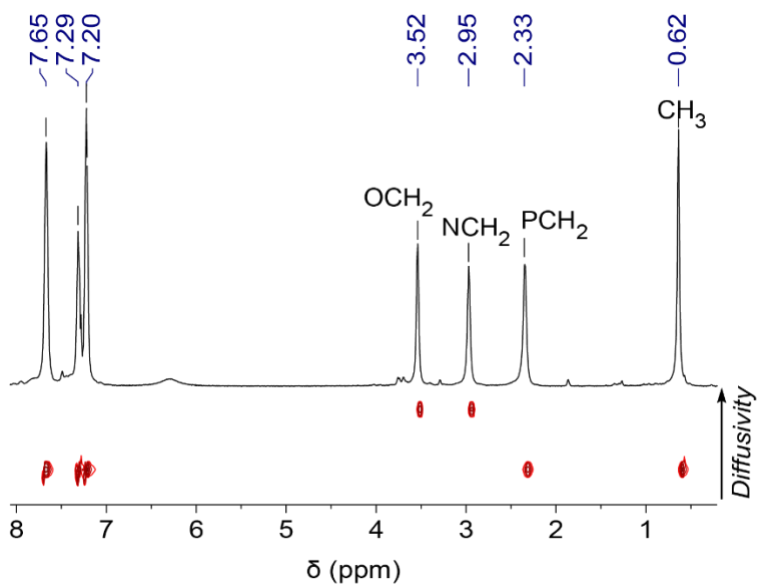


Figure s5. DOSY ^1H NMR plot (500 MHz, CDCl_3) of $1 \cdot (\text{Hc}^+\text{I}^-)_3$.

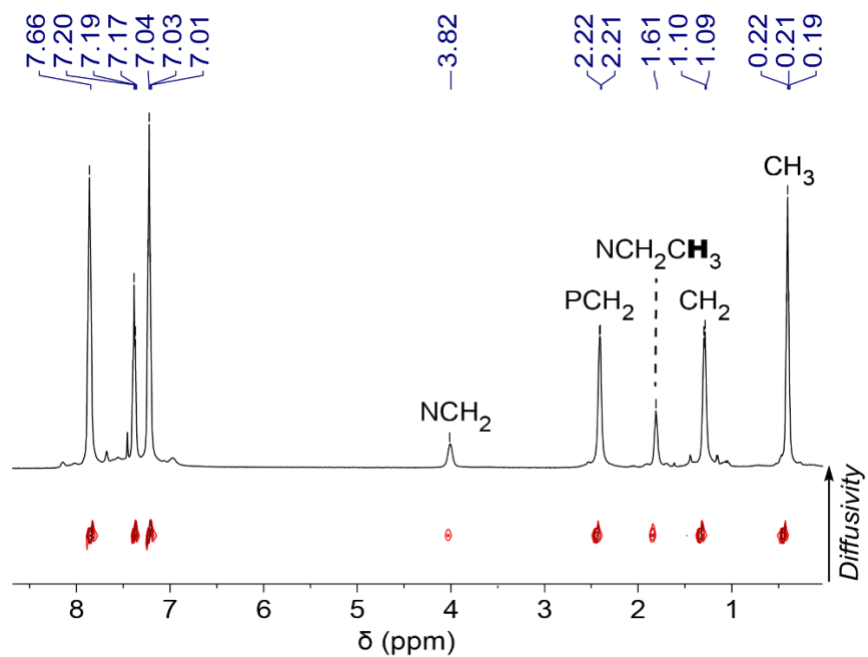


Figure s6. DOSY ^1H NMR plot (500 MHz, CDCl_3) of $2 \cdot \text{Ha}^+\text{I}^-$ (full version, Figure 3 in main text).

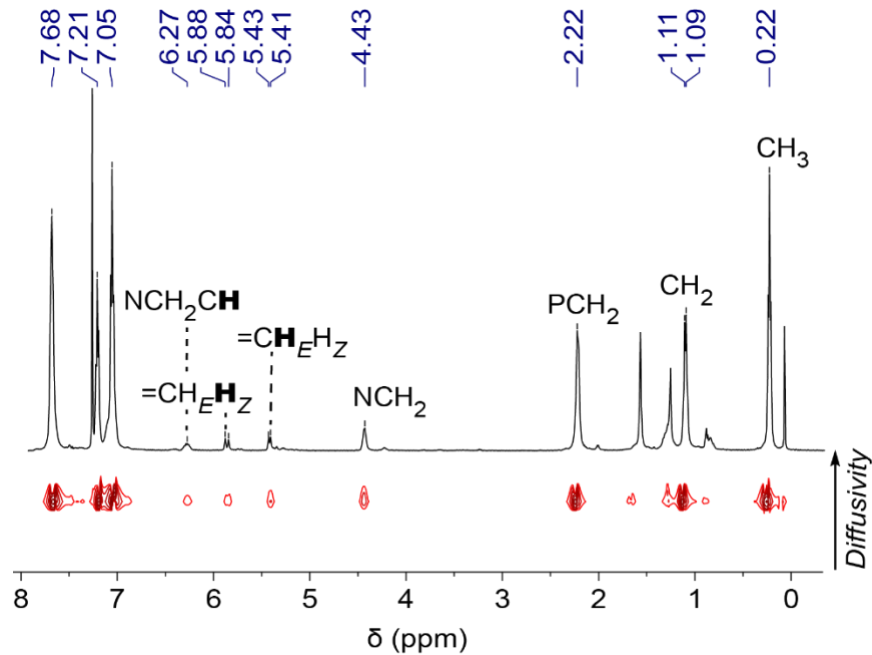


Figure s7. DOSY ^1H NMR plot (500 MHz, CDCl_3) of $2 \cdot \text{Hb}^+\text{I}^-$.

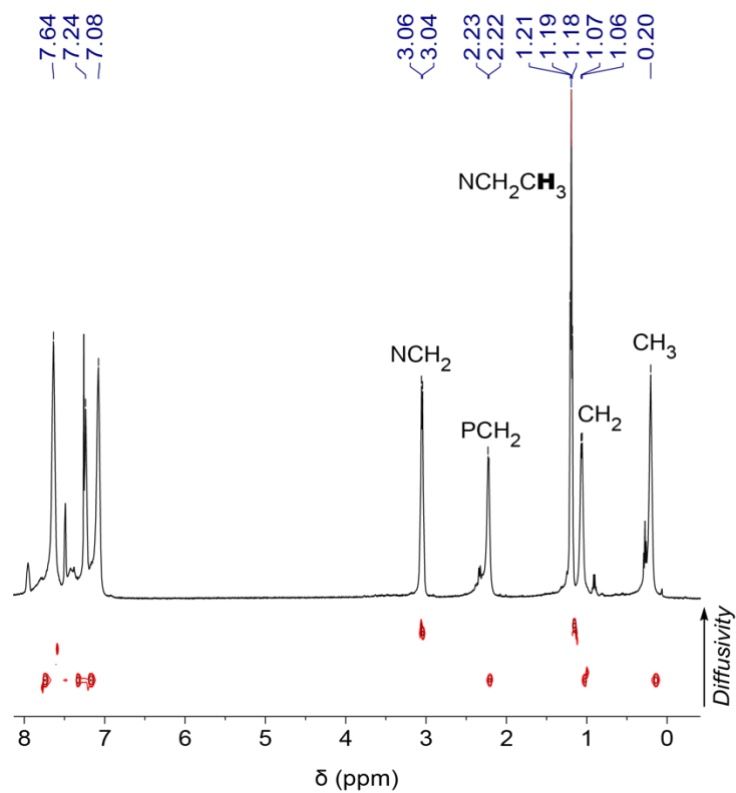


Figure s8. DOSY ^1H NMR plot (500 MHz, CDCl_3) of $2 \cdot (\text{Hd}^+\text{I})_3$.

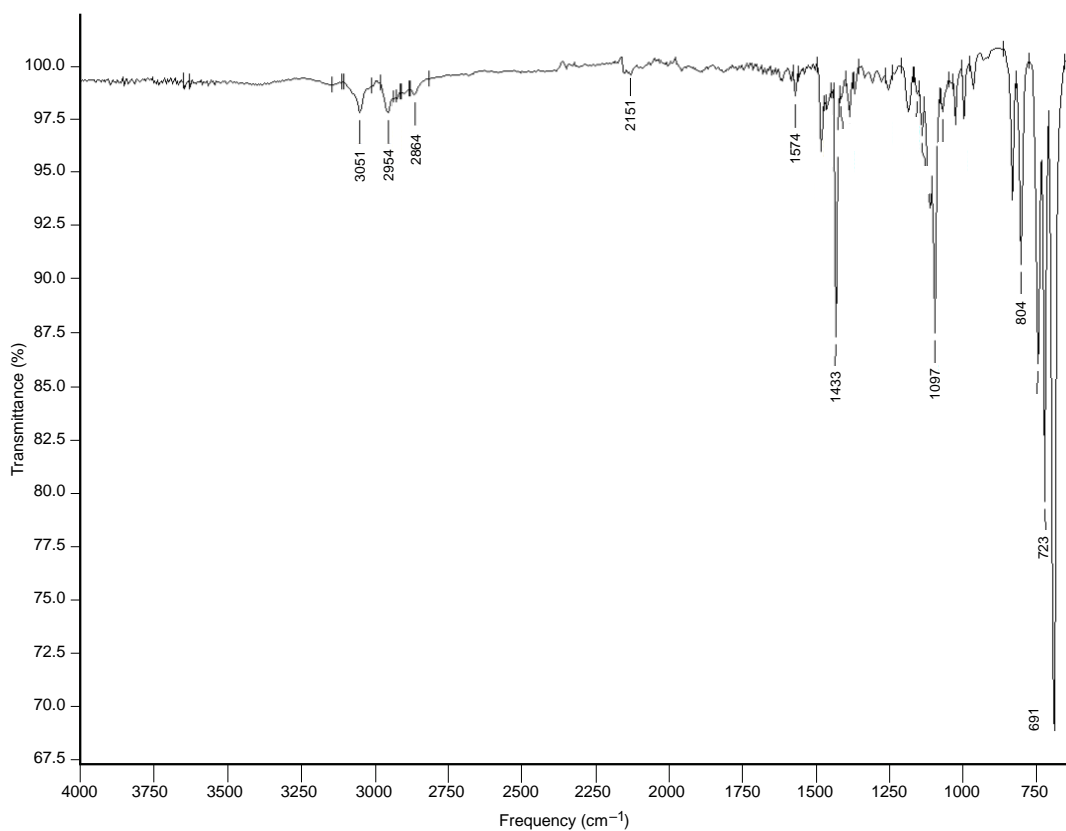


Figure s9. Representative IR spectrum ($1 \cdot \text{Ha}^+\text{I}$).

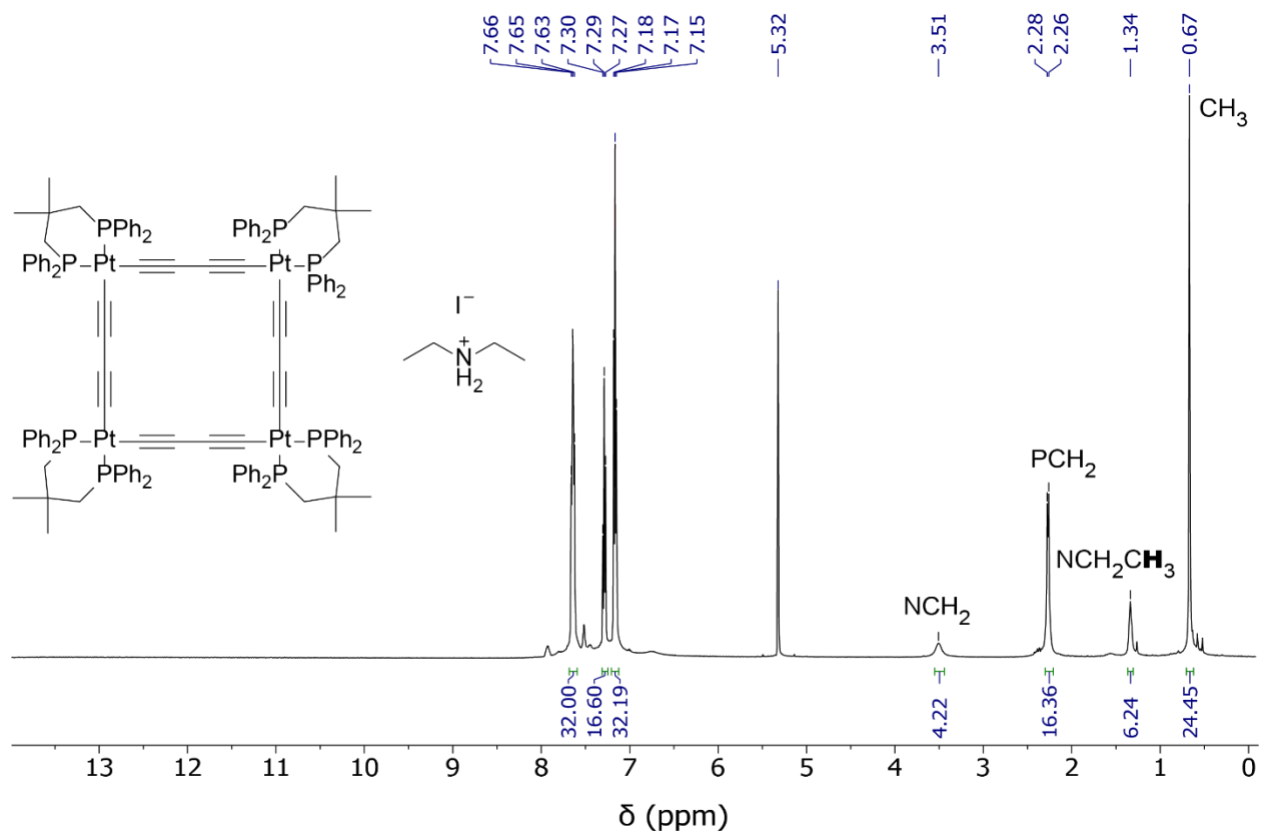


Figure s10. ^1H NMR spectrum of $1 \cdot \text{Ha}^+\text{I}^-$ (CD_2Cl_2 , 500 MHz).

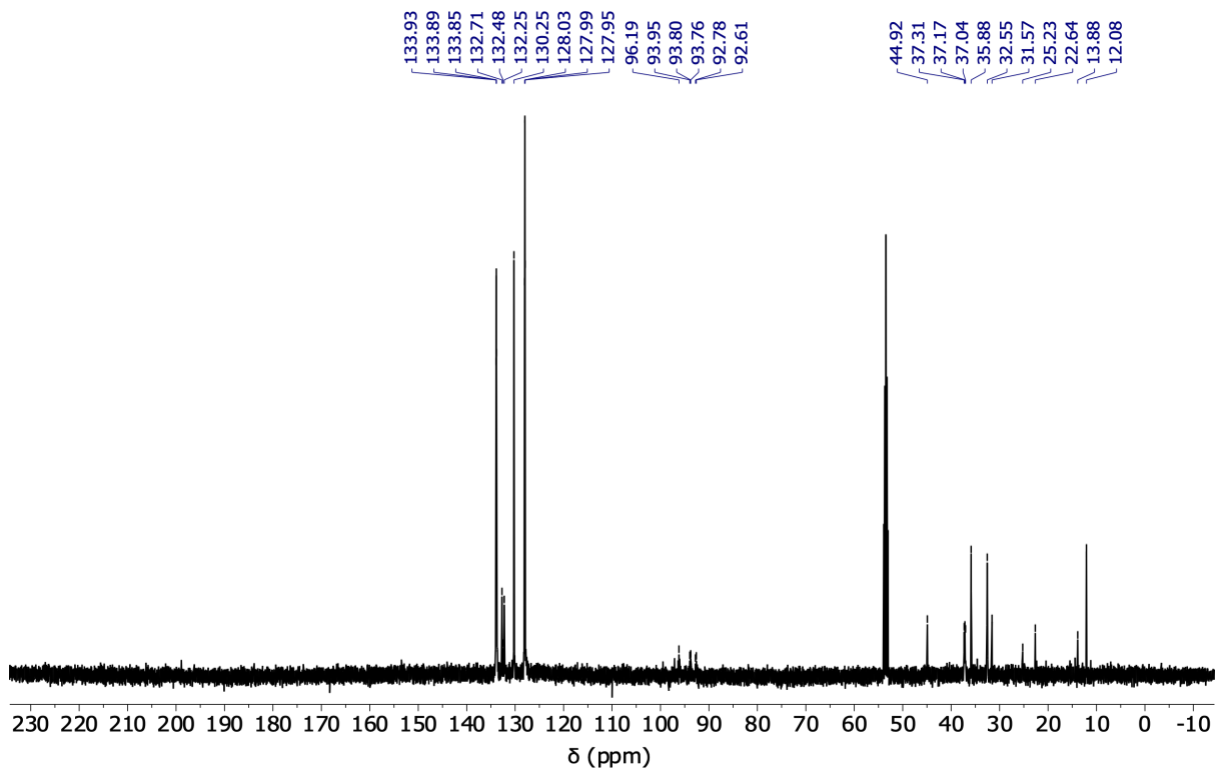


Figure s11. $^{13}\text{C}\{^1\text{H}\}$ NMR spectrum of $1 \cdot \text{Ha}^+\text{I}^-$ (CD_2Cl_2 , 101 MHz).

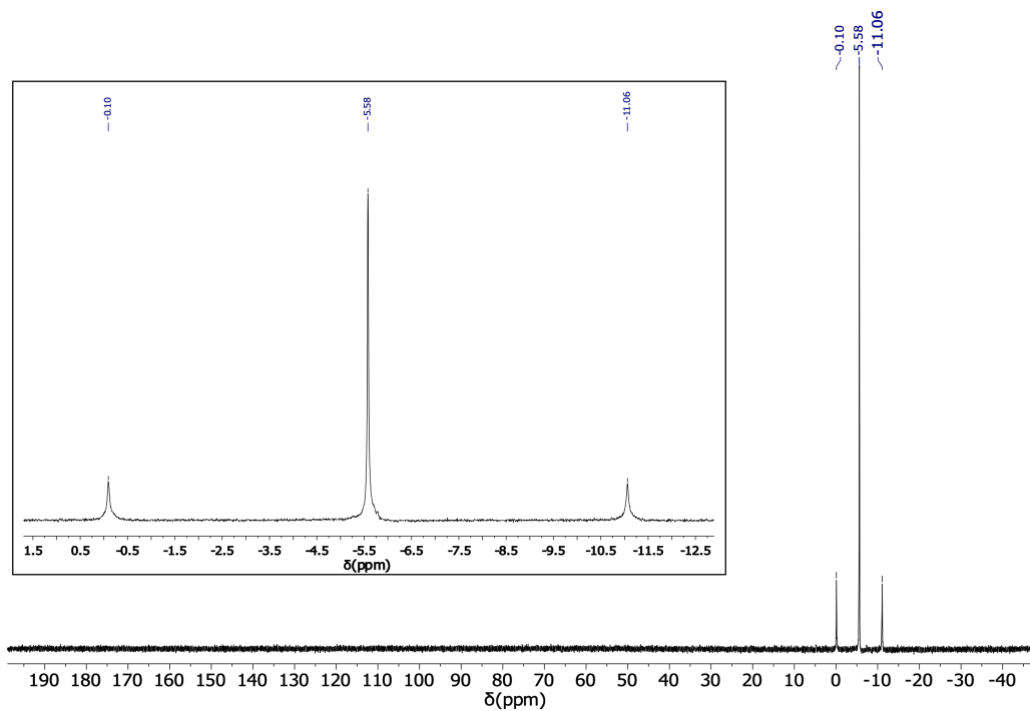


Figure s12. $^{31}\text{P}\{^1\text{H}\}$ NMR spectrum of $1 \cdot \text{Ha}^+\text{I}^-$ (CD_2Cl_2 , 202 MHz).

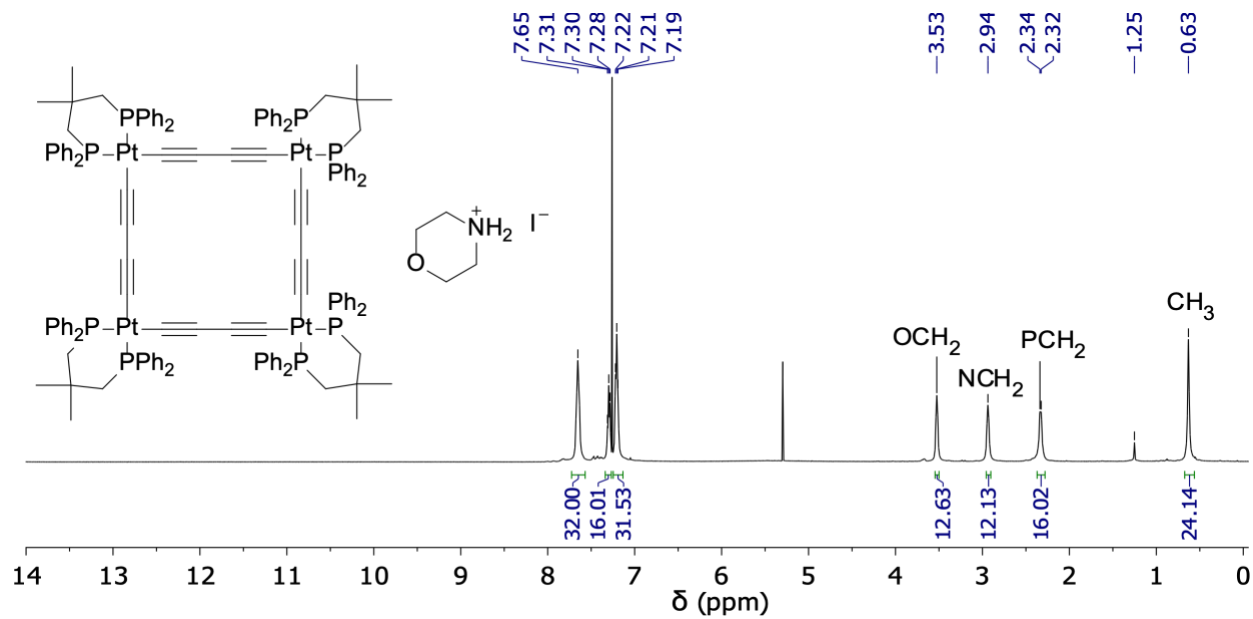


Figure s13. ^1H NMR spectrum of $1 \cdot (\text{Hc}^+\text{I}^-)$ (CDCl_3 , 500 MHz).

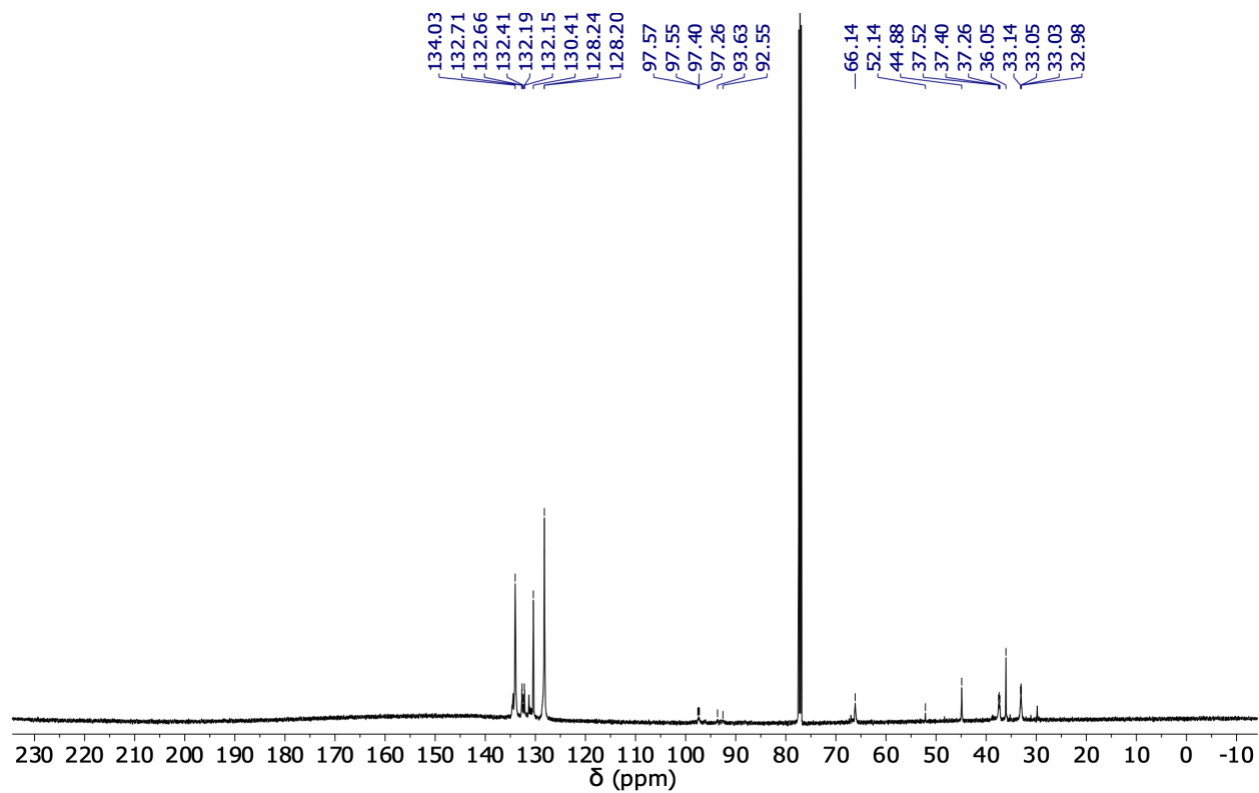


Figure s14. $^{13}\text{C}\{^1\text{H}\}$ NMR spectrum of $1 \cdot (\text{Hc}^+\text{I}^-)_3$ (CDCl_3 , 101 MHz).

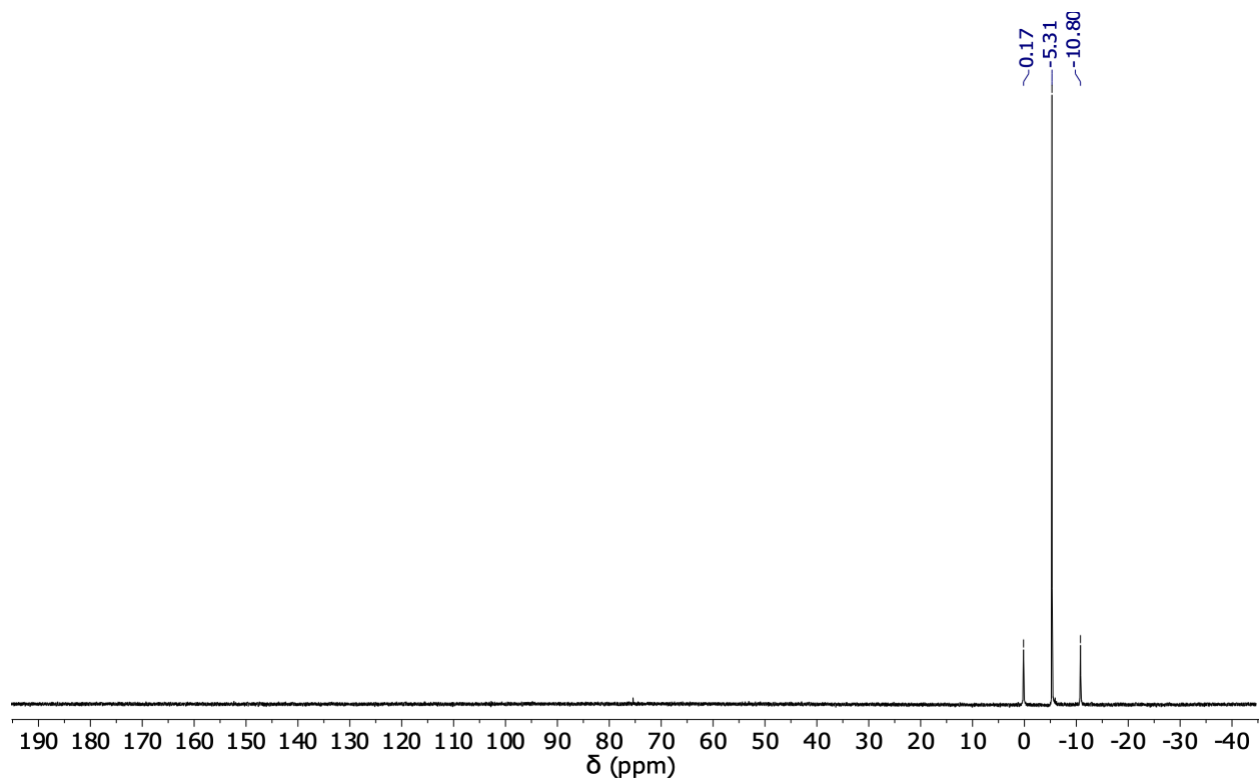


Figure s15. $^{31}\text{P}\{^1\text{H}\}$ NMR spectrum of $1 \cdot (\text{Hc}^+\text{I}^-)_3$ (CDCl_3 , 202 MHz).

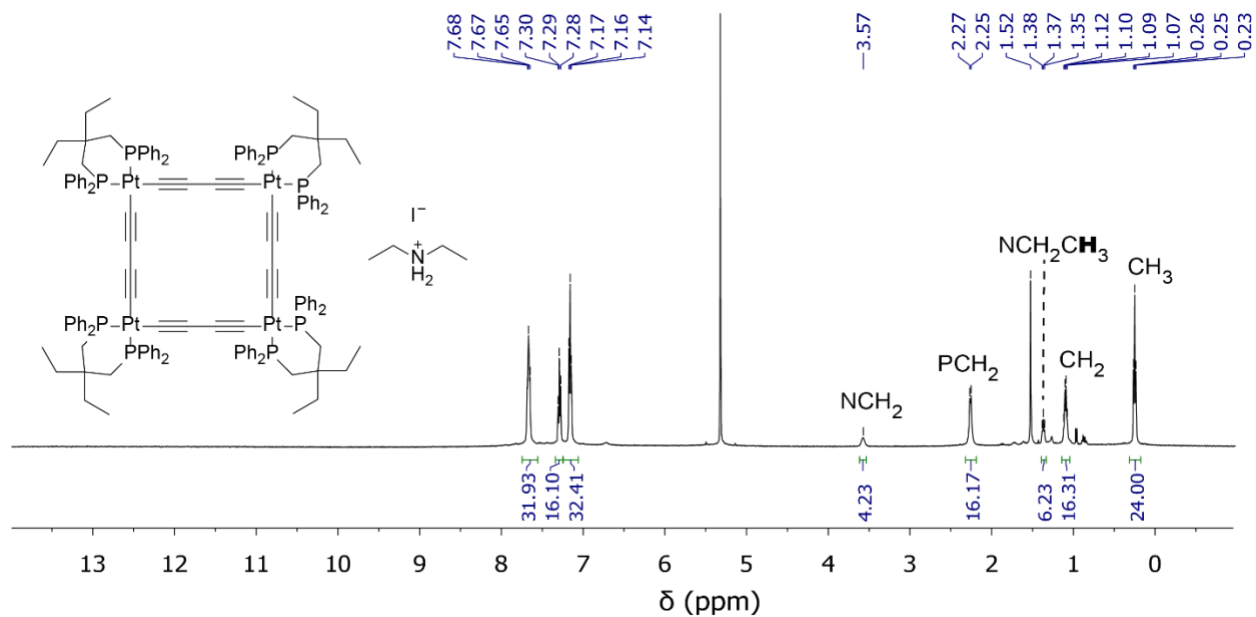


Figure s16. ^1H NMR spectrum of $2 \cdot \text{Ha}^+\text{I}^-$ (CD_2Cl_2 , 500 MHz).

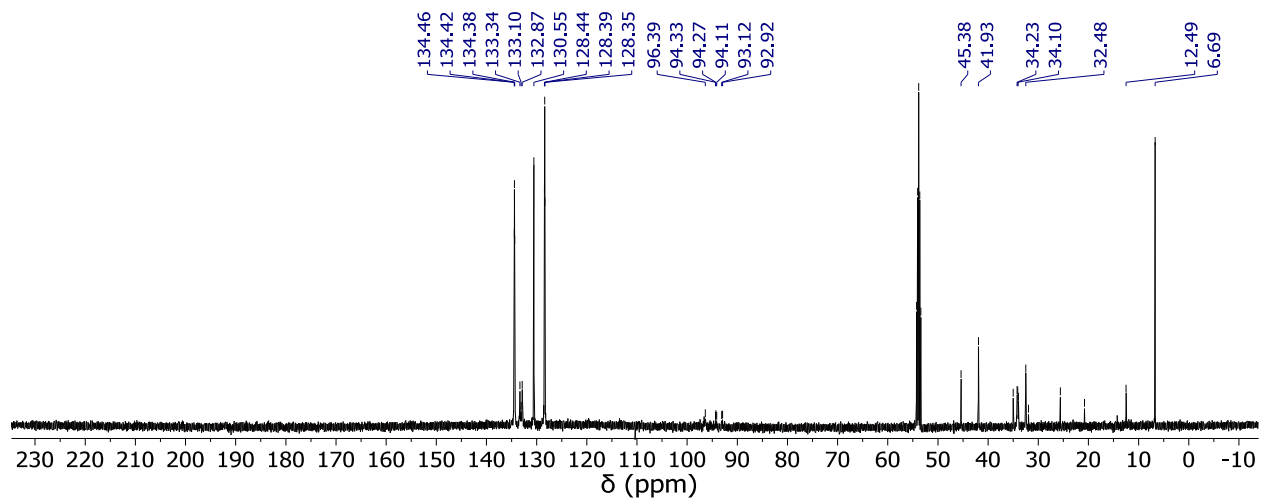


Figure s17. $^{13}\text{C}\{^1\text{H}\}$ NMR spectrum of $2 \cdot \text{Ha}^+\text{I}^-$ (CD_2Cl_2 , 101 MHz).

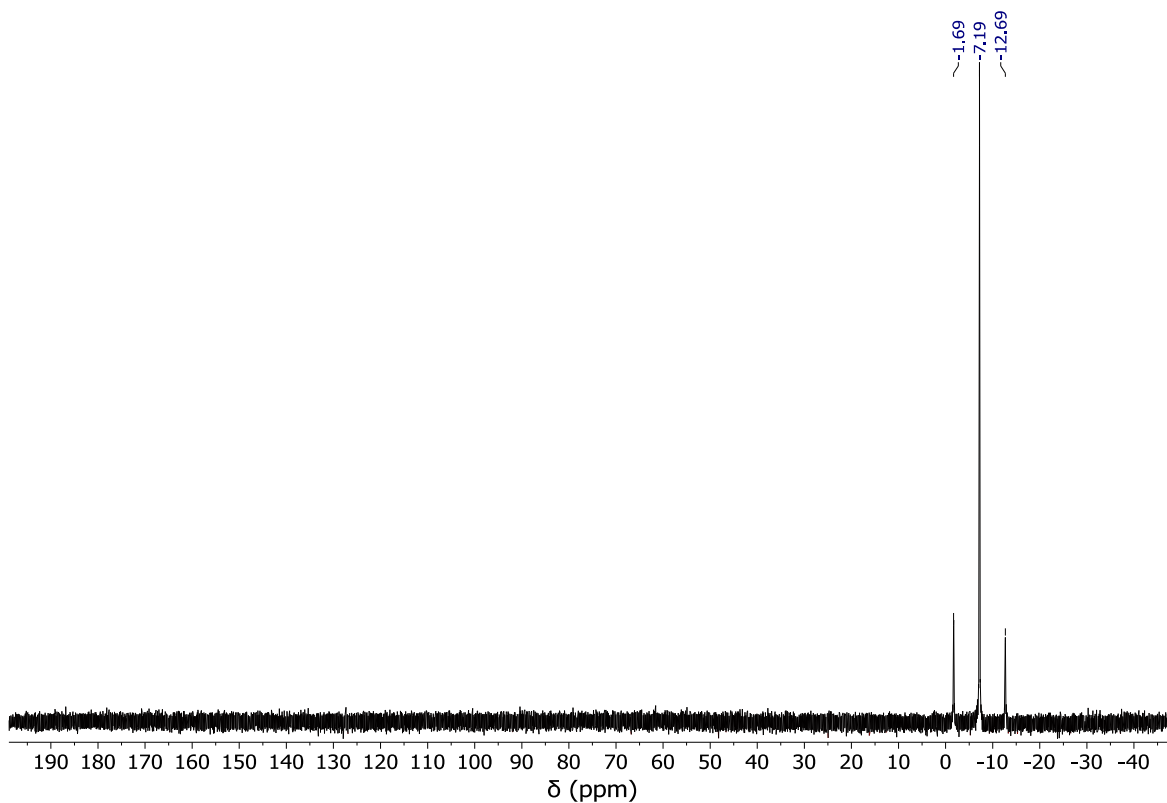


Figure s18. $^{31}\text{P}\{^1\text{H}\}$ NMR spectrum of $2 \cdot \text{Ha}^+\text{I}^-$ (CD_2Cl_2 , 202 MHz).

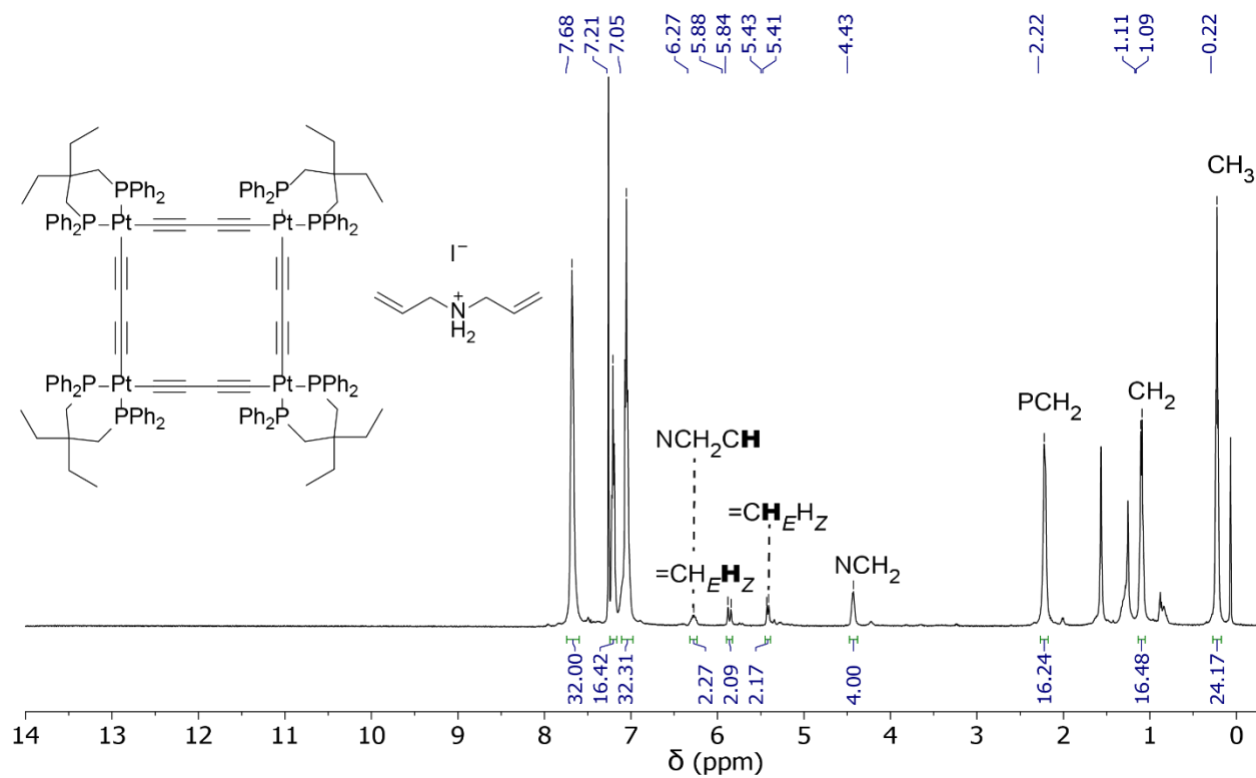


Figure s19. ^1H NMR spectrum of $2 \cdot \text{Hb}^+\text{I}^-$ (CDCl_3 , 500 MHz).

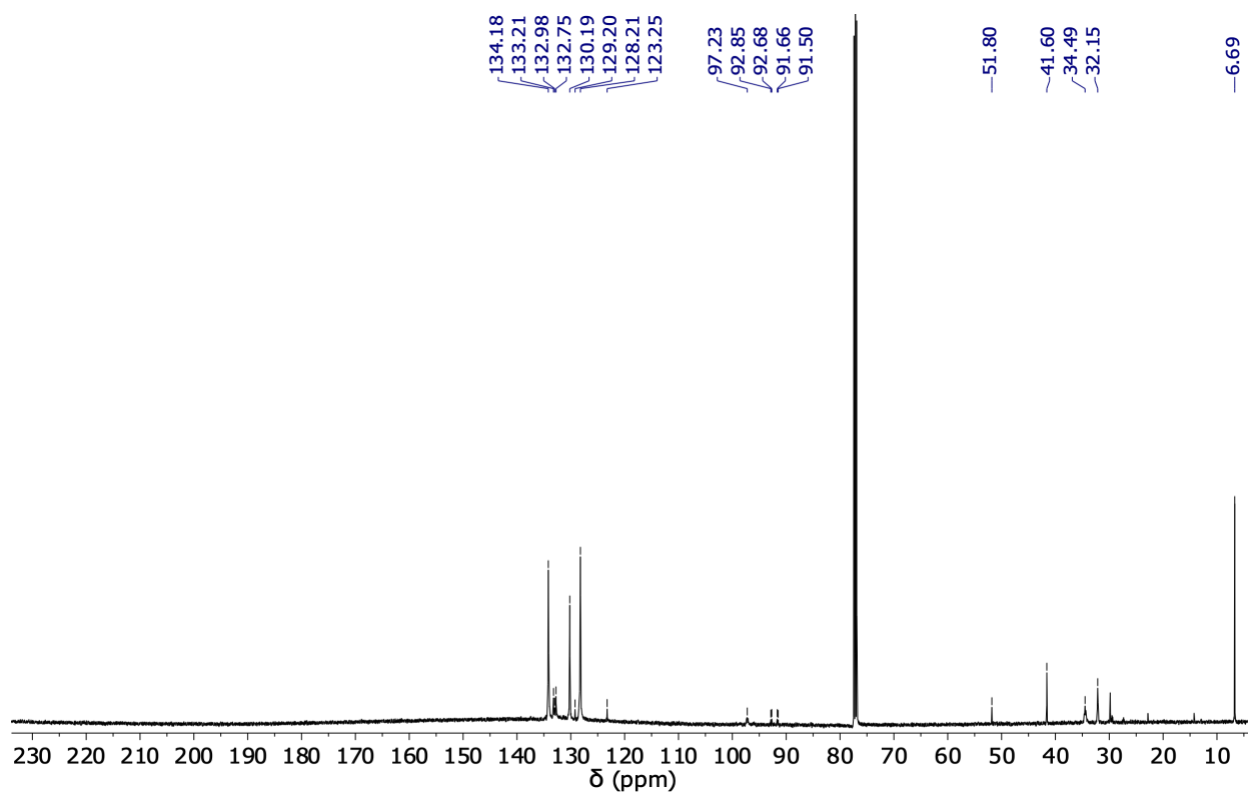


Figure s20. $^{13}\text{C}\{^1\text{H}\}$ NMR spectrum of $2\cdot\text{Hb}^+\text{T}^-$ (CDCl_3 , 101 MHz).

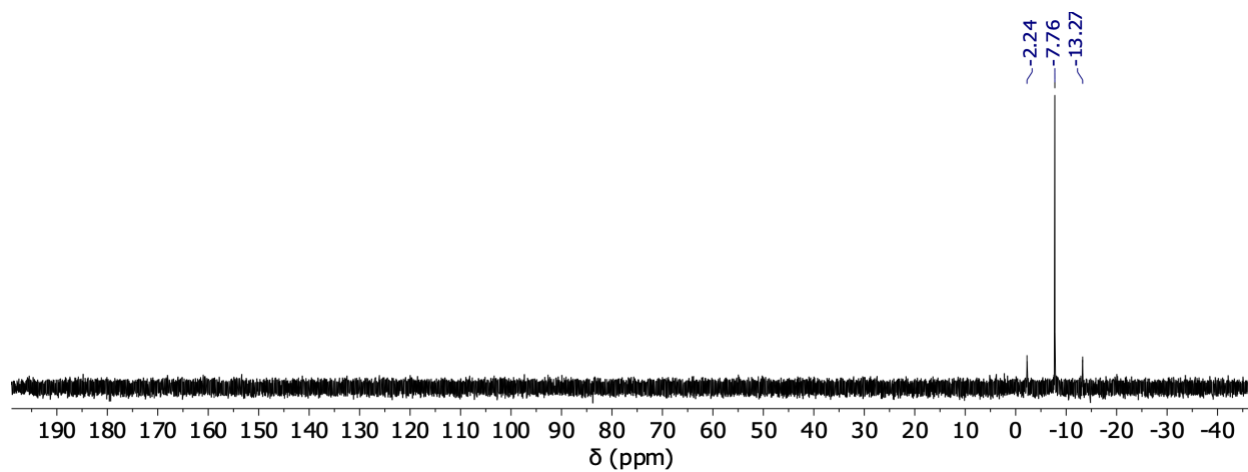


Figure s21. $^{31}\text{P}\{^1\text{H}\}$ NMR spectrum of $2\cdot\text{Hb}^+\text{T}^-$ (CDCl_3 , 202 MHz).

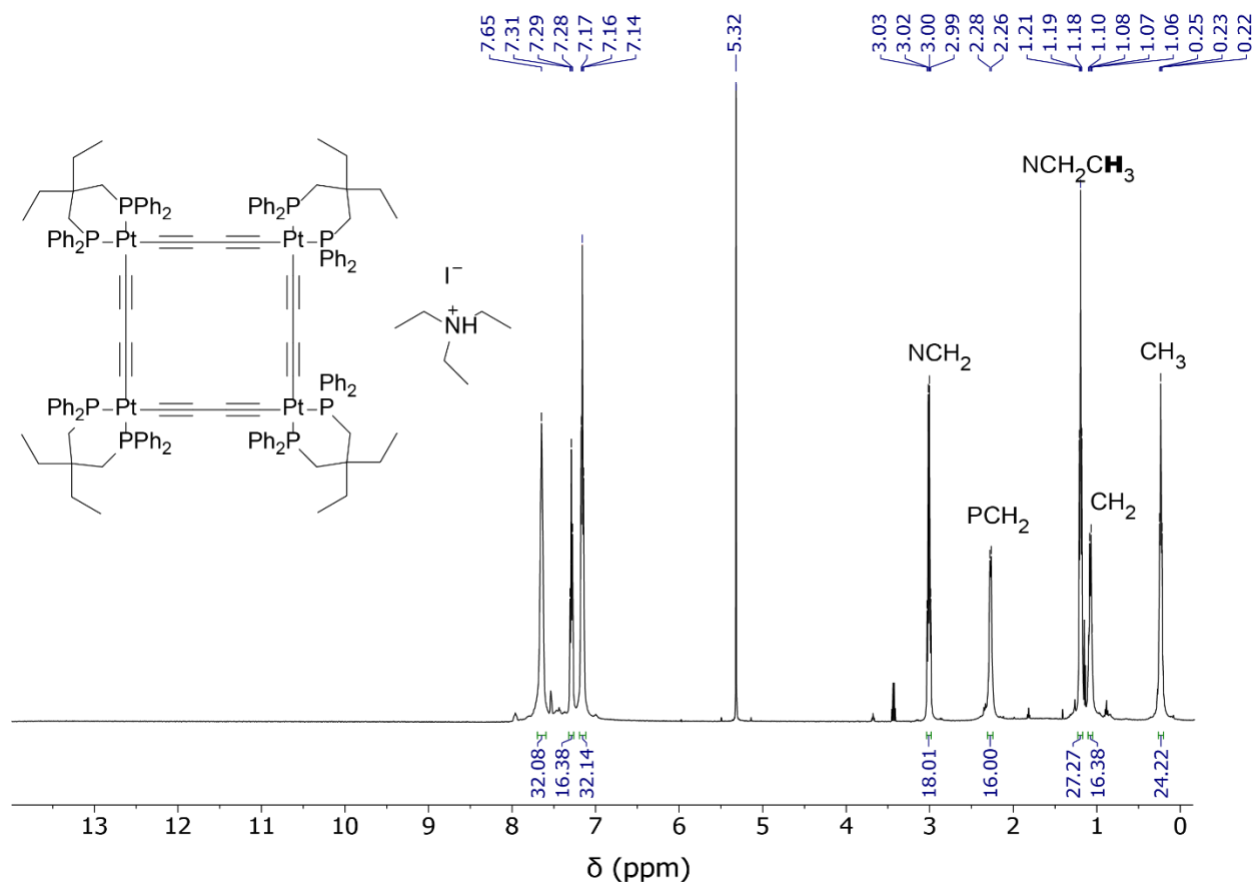


Figure s22. ^1H NMR spectrum of $2 \cdot (\text{Hd}^+\text{I}^-)_3$ (CD_2Cl_2 , 500 MHz).

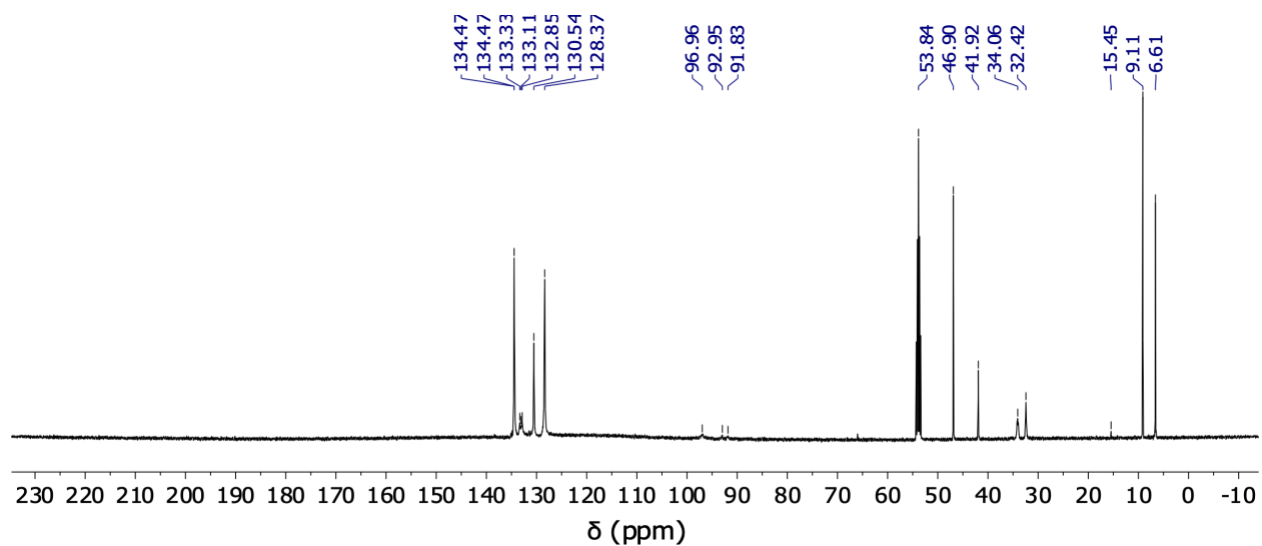


Figure s23. $^{13}\text{C}\{^1\text{H}\}$ NMR spectrum of $2 \cdot (\text{Hd}^+\text{I}^-)_3$ (CD_2Cl_2 , 101 MHz).

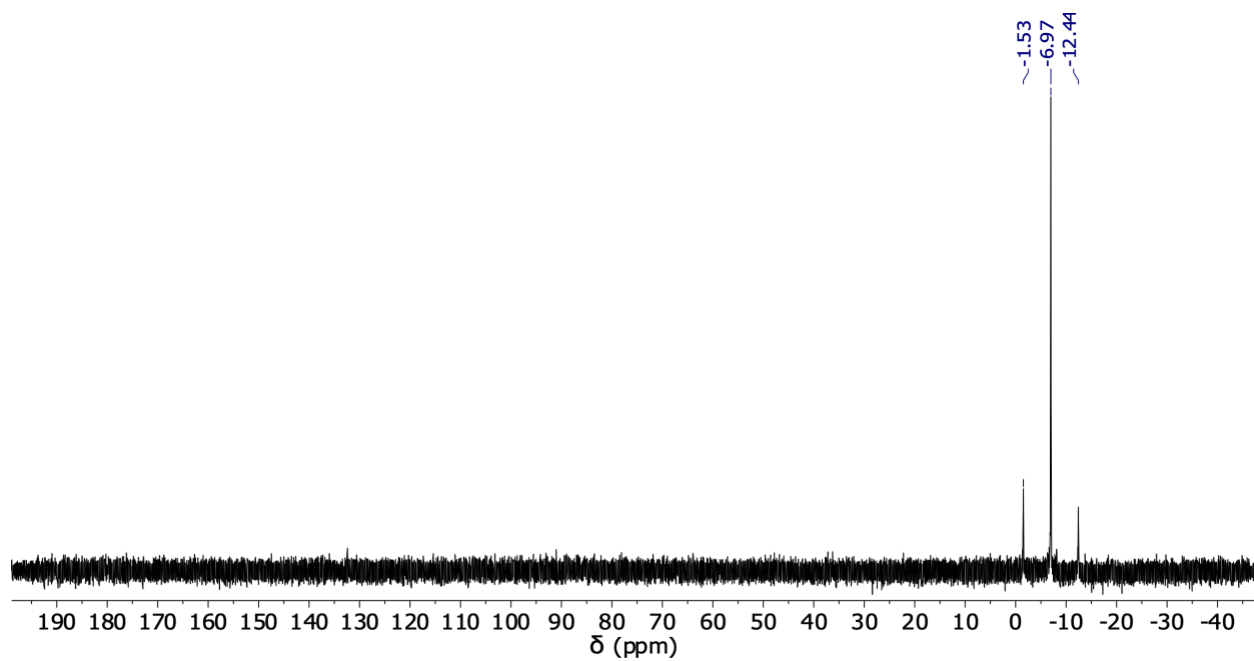


Figure s24. $^{31}\text{P}\{^1\text{H}\}$ NMR spectrum of $2 \cdot (\text{Hd}^+\Gamma)_3$ (CD_2Cl_2 , 202 MHz).